Strong binding and shrinkage of single and double $\bar{K}$ nuclear systems
(K^-pp, K^-ppn, K^-K^-p and K^-K^-pp)
predicted by Faddeev-Yakubovsky calculations

By Shuji MAEDA,[*1] Yoshinori AKAISHI[*2,*3] and Toshimitsu YAMAZAKI[*2,*4,†]

(Contributed by Toshimitsu YAMAZAKI, M.J.A.)

Abstract: Non-relativistic Faddeev and Faddeev-Yakubovsky calculations were made for K^-pp, K^-ppn, K^-K^-p and K^-K^-pp kaonic nuclear clusters, where the quasi bound states were treated as bound states by employing real separable potential models for the K^--K^- and the K^--nucleon interactions as well as for the nucleon-nucleon interaction. The binding energies and spatial shrinkages of these states, obtained for various values of the $\bar{K}N$ interaction, were found to increase rapidly with the $\bar{K}N$ interaction strength. Their behaviors are shown in a reference diagram, where possible changes by varying the $\bar{K}N$ interaction in the dense nuclear medium are given. Using the $\Lambda(1405)$ ansatz with a PDG mass of $1405\,\mathrm{MeV}/c^2$ for K^-p, the following ground-state binding energies together with the wave functions were obtained: $51.5\,\mathrm{MeV}$ (K^-pp), $69\,\mathrm{MeV}$ (K^-ppn), $30.4\,\mathrm{MeV}$ (K^-K^-p) and $93\,\mathrm{MeV}$ (K^-K^-pp), which are in good agreement with previous results of variational calculation based on the Akaishi-Yamazaki coupled-channel potential. The K^-K^-pp state has a significantly increased density where the two nucleons are located very close to each other, in spite of the inner NN repulsion. Relativistic corrections on the calculated non-relativistic results indicate substantial lowering of the bound-state masses, especially of K^-K^-pp, toward the kaon condensation regime. The fact that the recently observed binding energy of K^-pp is much larger (by a factor of 2) than the originally predicted one may infer an enhancement of the $\bar{K}N$ interaction in dense nuclei by about 25% possibly due to chiral symmetry restoration. In this respect some qualitative accounts are given based on "clearing QCD vacuum" model of Brown, Kubodera and Rho.

Keywords: kaonic nuclear few-body systems with shrinkage, double kaonic nuclei, Faddeev-Yakubovsky method, chiral symmetry restoration, high-density strange nuclei and matter

I. Introduction

For the past decade we have studied deeply bound and dense kaonic nuclear cluster (KNC) states using an empirically based coupled-channel $\bar{K}N$ complex potential,[1)–7)] which is characterized by a strongly attractive $I = 0$ $\bar{K}N$ interaction coupled with the $\Sigma\pi$ channels. Its strength was adjusted to reproduce the mass $1405\,\mathrm{MeV}/c^2$ for the so-called $\Lambda(1405)$, which was assumed as the quasi-bound K^--p state (called $\Lambda^* \equiv \Lambda(1405)$ ansatz). The most spectacular prediction, first shown in ref. 1, is that light nuclei involving a $\bar{K}$ as a constituent are shrunk to dense baryonic objects with densities nearly 3-times as much as the normal nuclear density. The structure of the most basic system, K^-pp, first predicted in 2002,[2)] was studied in detail by a realistic three-body calculation,[6),7)] and hence a molecular covalent nature of the strong binding was revealed. The K^-pp system was shown to have a structure of Λ^*-p, where the quasi-bound $I = 0$ $\bar{K}N$ pair that is identified as $\Lambda^* \equiv \Lambda(1405)$ behaves like an "atom". This study led us to a new concept of nuclear force, "super-strong nuclear force", which is caused by a real

*1   Department of Agro-Environmental Science, Obihiro University of Agriculture and Veterinary Medicine, Hokkaido, Japan.
*2   RIKEN Nishina Center, Saitama, Japan.
*3   College of Science and Technology, Nihon University, Chiba, Japan.
*4   Department of Physics, University of Tokyo, Tokyo, Japan.
†   Correspondence should be addressed: T. Yamazaki, RIKEN Nishina Center, 2-1, Hirosawa, Wako, Saitama 351-0198, Japan (e-mail: yamazaki@nucl.phys.s.u-tokyo.ac.jp).

$\bar{K}$ migrating between two nucleons, conceptually similar to the covalent bonding in hydrogen molecules: H_2^+ and H_2,[8] and has a binding strength nearly 4-times as large as that of the ordinary nuclear force. The uniqueness of this bonding is that it is caused by a strongly interacting real boson, $\bar{K}$. This new type of force was given a name by Nishijima:[9] "kaonic origin of nuclear force", which is contrasted to the ordinary "pionic origin of the nuclear force".

In these papers[6),7)] we have predicted a new formation mechanism of $K^- pp$ in the process of $pp \rightarrow K^+ + p + \Lambda^* \rightarrow K^+ + K^- pp$, whereas a normal Λ particle is produced in $pp \rightarrow K^+ + p + \Lambda$. The pp collision at high energy is known to produce $\Lambda(1405)$ among other hyperons, as revealed in missing-mass spectra, $MM(pK^+)$.[10),11)] It was theoretically clarified that the produced Λ^* serves as a doorway to form a complex Λ^*-$p \approx K^- pp$. This sticking process occurs strongly when the formed $K^- pp$ has a small p-p distance that matches the small proximity of the pp collision with a short collision length of ~ 0.3 fm, helped by a large momentum transfer of ~ 1.6 GeV/c at $T_p \sim 3$ GeV. In other words, the doorway particle, Λ^*, sticks to the participating p at an enormously high probability to form a $K^- pp$, if and only if it is dense, and thus the occurrence of this reaction with a large $K^- pp$ cross section would provide definite evidence for a dense $\bar{K}$ nuclear state. Thus, the pp reaction has a great advantage for KNC production compared to statistical coalescence processes where deeply bound and dense states are hardly formed.[12)]

Recently, this pp reaction process was searched for in old DISTO experimental data of exclusive events of $pp \rightarrow p + \Lambda + K^+$ at $T_p = 2.85$ GeV, and the process was indeed found to take place.[13)] (An indication of $K^- pp$ had been reported before from a stopped-K^- experiment on light nuclei with a similar binding energy.[14)]) A broad peak showing $M = 2267 \pm 2(stat) \pm 5(syst)$ MeV/c^2 was revealed with as much intensity as the free Λ^* emission. The Λ^* production observed at large angles of proton emission in $pp \rightarrow p + K^+ + \Lambda^*$ reactions[15),16)] indicates that the Λ^* production takes place in a short collision length of pp,[17)] justifying the basis of our proposal. Thus, this experiment has indicated that the state observed is a dense $K^- pp$. In addition, the same reaction was studied at $T_p = 2.5$ GeV, a substantially lower energy compared with 2.85 GeV. The same $K^- pp$ with $M = 2267$ MeV/c^2 was expected kinematically, but it was not populated at 2.5 GeV.[15),18)] We have reached the following conclusion. At this lowered incident energy the Λ^*

production was very much decreased toward the production threshold, so that the production of $K^- pp$ through Λ^* sticking was also suppressed. In this way, the role of Λ^* as a doorway to form $K^- pp$ was understood. The observed binding energy of $K^- pp$ in DISTO is much larger than the original prediction of refs. 5, 7. Indeed, a view with a 25% enhancement over the original $\bar{K}N$ interaction seems to be compatible with the DISTO observation. We call this enhanced empirical interaction "DISTO". This fact strongly suggests that we have to consider seriously possible enhancement effects of the $\bar{K}N$ interaction in dense KNC systems.

The simplest double $\bar{K}$ nuclei, $K^- K^- pp$ and $K^- K^- ppn$, were also predicted to be deeply bound with binding energies of 117 MeV and 221 MeV, respectively.[5)] Extending the predicted and proven mechanism of a large sticking of Λ^* to p, we proposed a similar formation mechanism for $K^- K^- pp$ via a double Λ^*-Λ^* doorway.[19),20)] The $K^- K^- pp$ is expected to be formed abundantly by pp collisions of an incident proton energy of about 7 GeV. Thus, the double $\bar{K}$ nuclei are within the reach of experimental studies in the near future at J-PARC and FAIR. It is extremely interesting to search for double-$\bar{K}$ nuclear clusters, since they may serve as precursors to kaon condensation.[21)–23)] In view of the DISTO data, the $\bar{K}N$ interaction, and thus the actual binding of $K^- K^- pp$, may be much stronger than in the original prediction.

On the other hand, there are serious theoretical discrepancies concerning KNC bindings, essentially coming from the different starting ansatzes, whether A) the $\Lambda(1405)$ mass is at the traditional "phenomenological" value, 1405 MeV/c^2,[24)–26)] or B) a "chiral weak" value, 1420 MeV/c^2 or more together with a double-pole structure (for instance, see ref. 27). The latter *Chiral* ansatz leads to a substantially shallow $\bar{K}N$ potential, and thus to kaonic states of small binding energies.[28)] Very recently, Barnea *et al.*[29)] made a hyperspherical harmonics calculation for the $K^- pp$, $K^- ppn$ and $K^- K^- pp$ systems based on the "chiral weak" interaction, and obtained very shallow bound states. Naturally, all of these binding energies are substantially smaller than our earlier predictions, based on the "strong regime" $\bar{K}N$ interaction.[1)–7)] We point out that there is no clear experimental evidence to support the "chiral weak" ansatz and predictions. Recent HADES data on $pp \rightarrow p + \Lambda^* + K^+$[16)] is also in favour of the strong regime with the PGD value.[17)]

In any case, we herewith introduce such a practical way as a "reference diagram" (explained

below) to evaluate the difference of binding energies and sizes of KNC for various $\bar{K}N$ interactions for comparing different theories on equal footing. A possible change of the $\bar{K}N$ interaction due to the shrinkage of KNC is studied from the view point of chiral symmetry restoration. Clear evidence for partial restoration of chiral symmetry in a nuclear medium has been obtained from deeply bound pionic states,[30]–[32] which indicates that the quark condensate that exists in the free πN interaction decreases by ∼30% at the normal nuclear density. A similar and much more dramatic effect is expected in the case of $\bar{K}$ nuclear clusters because of the attractive character of the interaction, and thus of a tremendously amplified nuclear shrinkage effect, which we discuss at the end of this paper.

Since the developments of the Faddeev[33] and the Faddeev-Yakubovsky[34] methods to solve the 3- and the 4-body Schrödinger equations, respectively, in the form of integral equations, they have been successfully applied in many regions of few body physics because of their nature to give rigorous wave functions under assumed two-body interactions. This is due to the appropriate division of the 3-body (4-body) t-matrix and accordingly of the wave function into the Faddeev (Faddeev-Yakubovsky) components, so that the rigorous derivation of the wave function is most straightfowardly achieved under separable 2-body potentials. It has also been clearly shown that the Faddeev-Yakubovsky calculation can have a high precision under local realistic potentials, as shown by a benchmark test calculation of a four-nucleon bound state.[35] Application of this method has been extended to the strangeness nuclear physics by Filikhin and Gal.[36] In the problem of $\bar{K}$-bound high-density nuclear systems, the Faddeev and the Faddeev-Yakubovsky methods should have an advantage to clarify the structure of the wave function in the central region of the system where more than two particles are very close to each other so that the wave function can be complicated, because, in contrast to the variational methods and the wave functional expansion methods like the hyperspherical harmonics method, they presuppose no structures of the wave function.

K^-pp has been treated by Shevchenko, Gal and Mares,[37] Shevchenko, Gal, Mares, and Révai,[38] and Ikeda and Sato[39]–[41] in the integral equation formalism. In these calculations, they used the Alt-Grassberger-Sandhas (AGS) equation[42] to find the resonance energies and widths. The AGS equation is directly connected to the scattering matrix elements

via the channel resolvents, and is thus fit to calculate reaction quantities, but is not directly connected to the wave function. This is the reason why these authors derived only the energies and widths of K^-pp. On the other hand, to study the shrinkage and formation of dense nuclear configurations inside the KNC systems induced by the strongly attractive $\bar{K}N$ interaction, deriving the wave functions of the KNC states is indispensable. In nuclear bound states it is a general feature that the bound-state energy arises as a strong cancellation between the kinetic energy and the potential energy, and since the dense structure of the system may be linked to a large kinetic energy expectation value, the calculation of this quantity from the wave function may contain important information about the shrinkage behavior of the KNC systems. In the present Faddeev and Faddeev-Yakubovsky calculations, we put emphasis on the derivation and detailed analysis of the wave functions.

II. Faddeev-Yakubovsky formalism

For systematic calculations of the ground-state energies and the density distributions of the light $\bar{K}$-nuclear systems, we performed 3-body and 4-body calculations with separable pair potentials in the non-relativistic Faddeev and Faddeev-Yakubovsky formalisms. In the Faddeev-Yakubovsky formalism, the bound-state wave function of a four-particle system Ψ is written as a sum of two kinds of components (Faddeev-Yakubovsky components) ψ and χ,

$$\Psi = \sum_{\alpha}^{12} \psi(\vec{k}_{\alpha}, \vec{p}_{\alpha}, \vec{q}_{\alpha}) + \sum_{\beta}^{6} \chi(\vec{k}_{\beta}, \vec{\kappa}_{\beta}, \vec{s}_{\beta}), \qquad [\text{II.1}]$$

where $(\vec{k}_{\alpha}, \vec{p}_{\alpha}, \vec{q}_{\alpha})$ and $(\vec{k}_{\beta}, \vec{\kappa}_{\beta}, \vec{s}_{\beta})$ are two kinds of sets of Jacobi momenta for the four-particle system, and α and β correspond to different choices of these sets of Jacobi momenta. It is well known that the Faddeev and the Faddeev-Yakubovsky components are rather simple in structure compared with the total wave functions. This would be a great advantage of the methods for such a calculation as the present one, where the different natures of the different pair interactions together with the strong binding would bring complex structures into the wave functions.

In the case of a separable S-wave two-body potential,

$$v(\vec{k}, \vec{k}') = \sum_{i} \lambda_i g_i(k) g_i(k') \frac{1}{4\pi}, \qquad [\text{II.2}]$$

the t-matrix is also an S-wave, and is written as

$$t(\vec{k}, \vec{k'}; z) = \sum_{ij} g_i(k) \tau_{ij}(z) g_j(k') \frac{1}{4\pi}$$

$$[\tau^{-1}(z)]_{ij} = \frac{1}{\lambda_i} \delta_{ij} - \int_0^\infty k^2 dk \frac{g_i(k) g_j(k)}{z - \frac{\hbar^2}{2\mu} k^2}, \quad [\text{II.3}]$$

where z is the two-body energy and μ is the reduced mass of the 2-body system. In this case, the Faddeev-Yakubovsky components are written in the form

$$\psi^\alpha(\vec{k}_\alpha, \vec{p}_\alpha, \vec{q}_\alpha) = \frac{1}{z - T^\alpha(k_\alpha, p_\alpha, q_\alpha)}$$
$$\times \sum_{ij} g_i^\alpha(k_\alpha) \tau_{ij}^\alpha(z - T^\alpha(p_\alpha, q_\alpha)) A_j^\alpha(\vec{p}_\alpha, \vec{q}_\alpha; z) \quad [\text{II.4}]$$

$$\chi^\beta(\vec{k}_\beta, \vec{\kappa}_\beta, \vec{s}_\beta) = \frac{1}{z - T^\beta(k_\beta, \kappa_\beta, s_\beta)}$$
$$\times \sum_{ij} g_i^\beta(k_\beta) \tau_{ij}^\beta(z - T^\beta(\kappa_\beta, s_\beta)) B_j^\beta(\vec{\kappa}_\beta, \vec{s}_\beta; z), \quad [\text{II.5}]$$

where z is the four-body energy, $T^\alpha(k_\alpha, p_\alpha, q_\alpha)$ and $T^\beta(k_\beta, \kappa_\beta, s_\beta)$ are the four-body kinetic energies represented by the Jacobi momenta, and $T^\alpha(p_\alpha, q_\alpha)$ and $T^\beta(\kappa_\beta, s_\beta)$ are the spectator kinetic energies. For a 2+2 system, there are 4 different functions, ψ^α, and 3 different functions, χ^β, while for a 3+1 system, there are 3 different functions, ψ^α, and 2 different functions, χ^β. A_j^α and B_j^β are solved by a set of coupled integral equations:

$$A_j^\alpha(\vec{p}_\alpha, \vec{q}_\alpha; z) = \sum_{j'j''\alpha'} \int d\vec{q}_{\alpha'}$$
$$\times X_{jj'}^{\alpha\alpha'}(\vec{p}_\alpha, \vec{p}_{\alpha'}; z - T^\alpha(q_\alpha)) \tau_{j'j''}^{\alpha'}(z - T^{\alpha'}(p_{\alpha'}, q_{\alpha'}))$$
$$\times A_{j''}^{\alpha'}(\vec{p}_{\alpha'}, \vec{q}_{\alpha'}; z) + \sum_{j'j''\beta'} \int d\vec{s}_{\beta'}$$
$$\times X_{jj'}^{\alpha\beta'}(\vec{p}_\alpha, \vec{\kappa}_{\beta'}; z - T^\alpha(q_\alpha)) \tau_{j'j''}^{\beta'}(z - T^{\beta'}(\kappa_{\beta'}, s_{\beta'}))$$
$$\times B_{j''}^{\beta'}(\vec{\kappa}_{\beta'}, \vec{s}_{\beta'}; z) \quad [\text{II.6}]$$

$$B_j^\beta(\vec{\kappa}_\beta, \vec{s}_\beta; z) = \sum_{j'j''\alpha'} \int d\vec{q}_{\alpha'}$$
$$\times Y_{jj'}^{\beta\alpha'}(\vec{\kappa}_\beta, \vec{p}_{\alpha'}; z - T^\beta(s_\beta)) \tau_{j'j''}^{\alpha'}(z - T^{\alpha'}(p_{\alpha'}, q_{\alpha'}))$$
$$\times A_{j''}^{\alpha'}(\vec{p}_{\alpha'}, \vec{q}_{\alpha'}; z), \quad [\text{II.7}]$$

where $X_{jj'}^{\alpha\alpha'}$ and $X_{jj'}^{\alpha\beta'}$ are the [3+1] subsystem amplitudes and $Y_{jj'}^{\beta\alpha'}$ are the [2+2] subsystem amplitudes, with $T^\alpha(q_\alpha)$ and $T^\beta(\beta)$ the spectator kinetic energies with respect to these subsystems.

We make a separable representation for these subsystem amplitudes by the energy dependent pole expansion (EDPE).[43] The convergence behavior of this expansion has been investigated in the bound states of the cluster of 4 helium atoms,[44] and found to be fast compared with that of the Hilbert-Schmidt expansion,[45] so that retaining only one term for each subsystem amplitude already achieves a good approximation. The system of 4 helium atoms was also treated by the Faddeev-Yakubovsky equation in configuration space by Filikhin *et al.* within the cluster expansion method,[46] and their value agreed with ours by the first two digits. In the present study, we retained only 1 term of EDPE for each subsystem amplitude, *i.e.*, the amplitude dominated by the subsystem ground state pole (EDPA).

For the 2-body potentials, we adopted S-wave separable potentials with Yamaguchi form factors:

$$\lambda_i = \frac{4}{\pi} \frac{\hbar^2}{2\mu} \frac{s_i}{\beta_i},$$
$$g_i(k) = \frac{\beta_i^2}{k^2 + \beta_i^2}, \quad [\text{II.8}]$$

where μ is the reduced mass of the 2-body system. For the NN potential we used the rank-2 potentials of Ikeda and Sato:[39]

$$^1S_0 \ (I=1): \quad s_R = 7.40, \ \beta_R = 6.157 \, \text{fm}^{-1},$$
$$s_A = -2.48, \ \beta_A = 1.784 \, \text{fm}^{-1},$$
$$^3S_1 \ (I=0): \quad s_R = 7.40, \ \beta_R = 6.157 \, \text{fm}^{-1},$$
$$s_A = -3.26, \ \beta_A = 1.784 \, \text{fm}^{-1}, \quad [\text{II.9}]$$

where suffixes R and A indicate the repulsive and attractive terms, respectively.

For the $\bar{K}N$ and $\bar{K}\bar{K}$ potentials we used rank-1 potentials:

$$\bar{K}N: \quad s_{(I=0)} = -1.37, \ \beta_{(I=0)} = 3.9 \, \text{fm}^{-1},$$
$$s_{(I=1)} = 0.29 \cdot s_{(I=0)}, \ \beta_{(I=1)} = \beta_{(I=0)},$$
$$\bar{K}\bar{K}: \quad s_{(I=1)} = 0.38, \ \beta_{(I=1)} = 3.9 \, \text{fm}^{-1}. \quad [\text{II.10}]$$

We call these short-ranged potentials the AMY (Akaishi-Myint-Yamazaki[47]) $\bar{K}N$ and $\bar{K}\bar{K}$ potentials. The range parameter values $3.9 \, \text{fm}^{-1}$ are adopted to represent the exchange of heavy mesons, like the ρ meson.

Among the $\bar{K}$ nuclear systems studied in the present work, the K^-K^-pp system is particularly an interesting system because it contains various features of interaction: a weakly repulsive interaction between the two anti-kaons, an interaction between the two nucleons with long-range attraction and short-range repulsion, and a short-range strong attraction between an $\bar{K}$ and a nucleon. We found that, among these, the $I = 0$ $\bar{K}N$ attraction plays a dominant role to determine the structure of the ground-state wave function.

The $\bar{K}N$ pair assumes two isospin states: $I = 0$ and $I = 1$. To incorporate these multi-state isospin configurations, we made a simplified treatment; we calculated the t-matrix in the $I = 0$ state with the $I = 0$ potential and the t-matrix in the $I = 1$ state with the $I = 1$ potential, and averaged these t-matrices with the weights $w = 0.75$ and $1 - w = 0.25$, respectively, for the K^-K^-p, K^-pp, K^-K^-pp systems, and $w = 0.5$ and $1 - w = 0.5$ for the K^-ppn system. It is expected that this treatment ("t-averaging" calculation) takes into account the strongly attractive $I = 0$ interaction more properly than averaging the $I = 0$ and $I = 1$ potentials and obtaining a t-matrix for the $\bar{K}N$ system by the averaged $\bar{K}N$ potential (V-averaging calculation). We followed a similar prescription for the NN configurations in the K^-ppn calculation. The t-matrix averaging Faddeev and Faddeev-Yakubovsky calculations have an advantage for systematic calculations, like the present study, because it is an easy way to incorporate multi-state pair interactions when the interaction in one state is very strong and the interaction in the other states is weak. This effect will be demonstrated below by comparisons between the results for the bound state energies obtained by the t-matrix averaging and by the potential averaging calculations.

From the obtained wave functions we calculated the density distributions of the pair distances and of the distances of the anti-kaons and the nucleons from the center of masses, in the K^-K^-p, K^-pp, K^-K^-pp and K^-ppn systems. We show the formula for the density distributions $\rho(r)$ of the pair distances in the 3-body $L = 0$ states, where L is the total orbital angular momentum, in eq. [II.11]. The formulas for the distance of particles from the c.m. of the hypernuclei and formulas for the 4-body $L = 0$ states were derived by a straightforward extension of this formula.

$$
\begin{aligned}
1 &= \langle \psi | \psi \rangle \\
&= \frac{2}{\pi} \int_0^\infty r^2 dr \int d\vec{k} \int d\vec{k}' \int d\vec{p} \\
&\quad \times \psi(\vec{k}\vec{p}) \psi(\vec{k}'\vec{p}) \sum_\lambda \frac{2\lambda + 1}{4\pi} j_\lambda(kr) j_\lambda(k'r) P_\lambda(\hat{k} \cdot \hat{k}') \\
&\equiv \int_0^\infty r^2 dr \rho(r).
\end{aligned}
\qquad [\text{II.11}]
$$

Here, ψ is the normalized 3-body wave function, which is expressed as a sum of 3 Faddeev components, while $\vec{k}$ and $\vec{p}$ are the Jacobi momenta. In the case of the 4-body systems, the wave functions are

represented as a sum of 18 Faddeev-Yakubovsky components given by three Jacobi momenta. The multiple integration was made in the Monte Carlo scheme.

The density distributions are expressed as a sum of the λ components, where λ is the orbital angular momenta of the pairs or of a particle relative to the c.m. of the remaining part of the KNC system. For the ground states of the systems studied in the present work, it is found that the components with $\lambda > 0$ are negligible, so we retain only the terms with $\lambda = 0$ in the present study.

III. Results and discussion

A. Comparison between t-averaging and V-averaging procedures. First, let us see the ground state energies of the K^-p, K^-K^-p, K^-pp, K^-ppn, and K^-K^-pp systems, as listed in Table 1, where the results obtained by the t-averaging calculations are compared with those by the V-averaging calculations.

Here, we can observe that the ground states of the K^-K^-p, K^-pp, K^-K^-pp and K^-ppn systems gain appreciable binding when we take the t-averaging procedure rather than the V-averaging procedure. This indicates the fact that the strong $\bar{K}N$ attraction in the $I = 0$ state is well taken into account in the t-averaging calculations. As a result, we obtained $-51.5\,\text{MeV}$ for the ground-state energy of the K^-pp system, which is more than a factor of 2 deeper than that we obtain in the V-averaging case.

In the early 1960's, just after the discovery of the $\Lambda(1405)$ resonance,[48),49)] following the prediction of a K^-p quasi-bound state by Dalitz and Tuan,[50)] Nogami investigated the possible existence of $\bar{K}NN$ bound states, and claimed that K^-pp may exist as a bound state with a binding energy of $B(K^-pp) = 11.5\,\text{MeV}$.[51)] Sometimes, this paper is referred to as the first prediction of the K^-pp bound state.[52),53)] However, such citations are theoretically inadequate.

Table 1. Comparison of the calculated ground-state energies between the t-averaging and V-averaging procedures

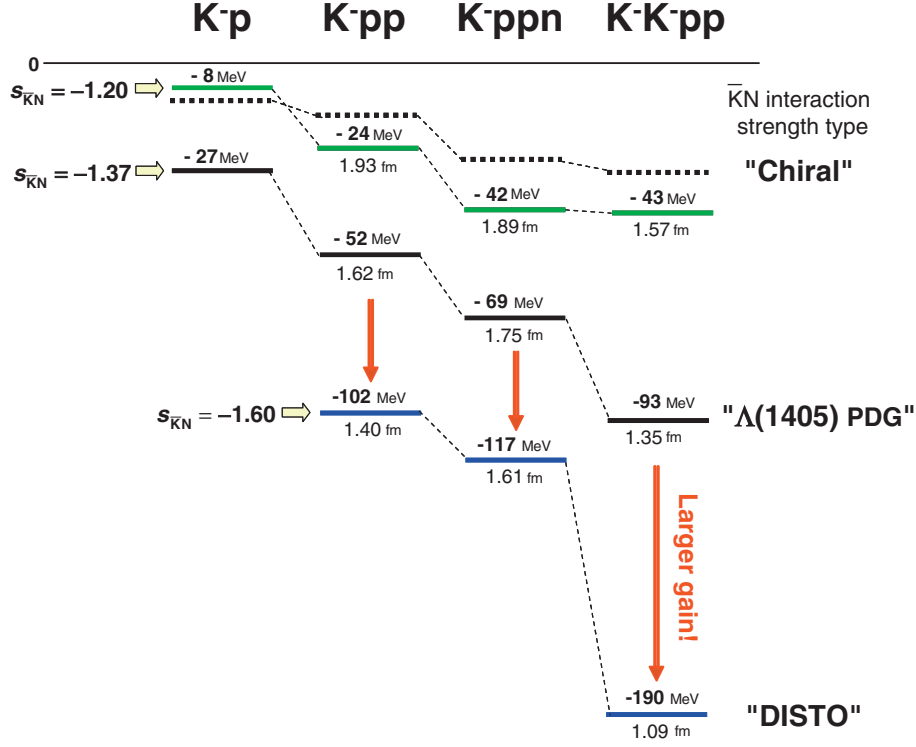| State	t-averaging	V-averaging
K^-p $(I = 0)$	$-26.6\,\text{MeV}$	$-26.6\,\text{MeV}$
K^-K^-p $(I = 1/2)$	$-30.4\,\text{MeV}$	$-5.0\,\text{MeV}$
K^-pp $(I = 1/2)$	$-51.5\,\text{MeV}$	$-23.6\,\text{MeV}$
K^-ppn $(I = 0)$	$-69\,\text{MeV}$	$-31\,\text{MeV}$
K^-K^-pp $(I = 0)$	$-93\,\text{MeV}$	$-54\,\text{MeV}$

Fig. 1. Global view of the calculated bound-state energies E_B (in MeV) and sizes R_{NN} (in fm) of $\bar{K}$ nuclear clusters, K^-p, K^-pp, K^-ppn and K^-K^-pp in the "Chiral" model ($s_{\bar{K}N}^{(I=0)} = -1.20$) (green bars) and in the "Standard" regime "$\Lambda(1405)$ PDG" ($s_{\bar{K}N}^{(I=0)} = -1.37$) (black bars) and an enhanced regime "DISTO" ($s_{\bar{K}N}^{(I=0)} = -1.60$) (blue bars). The chiral-based calculations of Barnea $et~al.$[29] are shown by black broken bars.

It should be noticed that the $B(K^-pp) = 11.5\,\text{MeV}$ is much less than $B(K^-p) = 29.9\,\text{MeV}$ that Nogami reproduced with his $\bar{K}N$ interaction; the K^-pp comes above the $\Lambda(1405) + p$ threshold. Thus, Nogami's K^-pp is not a bound state at all, and its escape width is estimated to be on the order of 300 MeV. Here, we have re-calculated the K^-pp system with Nogami's $\bar{K}N$ interaction using the same V-averaging treatment, which yielded a K^-pp bound state with $B(K^-pp) = 60.3\,\text{MeV}$. We have found that this K^-pp lies much more deeply than his state with $B(K^-pp) = 11.5\,\text{MeV}$. (Since his potential is of long range (two-π range), the V-averaging value is not so different from the t-averaging one.) Nogami's paper fatally missed just this genuine K^-pp ground state. After many years, the first prediction of K^-pp quasi-bound state below the $\Lambda(1405) + p$ threshold was given in 2002 by Yamazaki and Akaishi.[2]

The first prediction of K^-pp energy was given to be $-47.7 - i30.6\,\text{MeV}$ based on a variational method of Akaishi[54] with the following strongly isospin dependent $\bar{K}N$ interactions;

$$V_{\bar{K}N}^{I=0}(r) = (-595.0 - i83.0) \exp[-(r/0.66\,\text{fm})^2]\,\text{MeV},$$
$$V_{\bar{K}N}^{I=1}(r) = (-175.0 - i105.0) \exp[-(r/0.66\,\text{fm})^2]\,\text{MeV}.$$
$$[\text{III.12}]$$

Here we show V-averaging and t-averaging results for this realistic K^-pp case in order to know the accuracy of our isospin averaging procedures. The V-averaging treatment gives an energy of $-33.9 - i29.9\,\text{MeV}$, where higher-order effects of the $V_{\bar{K}N}^{I=0}$ strong attraction are improperly suppressed by the averaging with the $V_{\bar{K}N}^{I=1}$ weaker attraction. Most of such improper suppression can be removed by calculating separately the $I=0$ and $I=1$ t-matrices which incorporate their higher-order effects respectively. By simulating the isospin average of both the t-matrices we have obtained the t-averaging energy of the K^-pp to be $-45.4 - i32.4\,\text{MeV}$, which becomes much closer to the original value, $-47.7 - i30.6\,\text{MeV}$. Thus, we can estimate the error of the t-averaging to be $2 \sim 3\,\text{MeV}$ for realistic K^-pp.

As for the K^-K^-p system, Kanada-En'yo and Jido[55] made a variational calculation by a Gaussian expansion method. They obtained a bound state

(with the ground state energy -36.0 MeV) slightly below the K^-p threshold (-30.6 MeV), when the Akaishi K^-p effective potential was employed. We obtained a similar result, $i.e.$, -30.4 MeV for the ground-state energy of the K^-K^-p system just below the K^-p threshold -26.6 MeV. It is noted that we could not obtain such a bound state of the K^-K^-p system by the V-averaging procedure.

Barnea $et\ al.$[29] made a hyperspherical harmonics calculation for the K^-pp, K^-K^-pp and K^-ppn systems using the shallow chiral interaction model with the self-consistent energy dependence taken into account. They reproduced the ground-state energies of the K^-p and K^-pp systems by Doté $et\ al$,[28] based on the shallow chiral model, and obtained the ground-state energies of the K^-K^-pp and K^-ppn systems around -30 MeV. On the other hand, our calculation, based on the "strong regime" $\bar{K}N$ interaction, leads to very deep ground-state energies, $i.e.$, -69 MeV and -93 MeV for the K^-ppn and K^-K^-pp systems, respectively. In particular, it should be noted that the addition of one nucleon to the K^-K^-p system gains -62 MeV, and the addition of one $\bar{K}$ to the K^-pp system gains -41 MeV to the ground-state energy. Figure 1 shows a comparison of the present calculations with the result of a chiral-based theory of Barnea $et\ al.$[29] (black broken bars). Whereas in the latter calculation the K^-pp through K^-K^-pp levels are shallow and nearly flat (around -30 MeV), our result with the standard strength of the $\bar{K}N$ interaction ($s_{\bar{K}N}^{(I=0)} = -1.37$) is characterized by a sudden drop of the K^-K^-pp energy. This behavior is more significant with the increase of the attractive interaction toward $s_{\bar{K}N}^{(I=0)} = -1.60$.

B. Overview of binding energies and sizes. The analysis of the DISTO experiment on $pp \rightarrow p + K^+ + \Lambda$ reactions showed a peak structure in the K^+ missing mass, $\Delta M(K^+)$, and $M(p\Lambda)$ invariant mass spectra, indicating a compact K^-pp state formed with a binding energy of 103 MeV.[19] The observed binding energy is much larger than the theoretical prediction based on the strong $\bar{K}N$ regime, and suggests that in dense nuclear matter, the $\bar{K}N$ interaction may become stronger than in free space. Thus, it is interesting to systematically investigate the binding of the $\bar{K}$-nuclear systems, when the $\bar{K}N$ interaction is changed.

Since the structure of $\bar{K}$ nuclear states totally depends on the assumed $\bar{K}N$ interaction, we calculated the ground-state energies and rms nuclear radii as functions of the interaction strength, $s_{\bar{K}N}^{(I=0)}$. Figure 2 shows the behaviors of the ground state

energies of the K^-p, K^-K^-p, K^-pp, K^-ppn and K^-K^-pp systems when $s_{\bar{K}N}^{(I=0)}$ is varied, while the ratio of $s_{\bar{K}N}^{(I=1)}$ to $s_{\bar{K}N}^{(I=0)}$ and the other potential parameters are fixed.

The interaction parameter that we adopt ranges from the weak chiral regime ($s_{\bar{K}N}^{(I=0)} \approx -1.2$), as given in many chiral theories,[27)–29)] and a much stronger regime of our hypothetical concern ($s_{\bar{K}N}^{(I=0)} \approx -1.5$, $-1.6, -1.7$), which may be required to account for experiments. The standard "PDG" value with $M(\Lambda^*) = 1405$ MeV/c^2 corresponds to

$$\text{"Standard"} : s_{\bar{K}N}^{(I=0)}(\text{Std}) = -1.37. \qquad \text{[III.13]}$$

In this way, we can overview any theoretical predictions and the present and future observations. In Table 2 and Fig. 2 we summarize our results.

It has been well known since the publication of ref. 1 that the strong attractive $\bar{K}N$ interaction makes the $\bar{K}$ bound system shrunk, despite the strong short-range NN repulsion. Since our calculation is capable of providing the wave functions, we calculated the rms radii of the bound nucleons, R_{KNC}, of each $\bar{K}$ nuclear cluster (KNC) from the obtained nucleon wave function as

$$R_{KNC}^{\text{point}} = \sqrt{\frac{\langle \sum_i^{n_N} (\vec{r}_i - \vec{r}_G)^2 \rangle}{n_N}}, \qquad \text{[III.14]}$$

where n_N is the number of the nucleons in the KNC system, $\vec{r}_i$ is the position of the i-th nucleon, $\vec{r}_G$ is the position of the center of mass of the KNC system, and the bracket $\langle \ \rangle$ denotes an expectation value with a normalized wave function of KNC. In the definition of R_{KNC}^{point}, each nucleon is assumed to be a point. Then, we convoluted the nucleon size from the known proton radius,[24]

$$r_p^{rms} = 0.88 \text{ fm}, \qquad \text{[III.15]}$$

into R_{KNC} to obtain an rms nuclear radius of

$$R_{KNC} = \sqrt{(R_{KNC}^{\text{point}})^2 + (r_p^{rms})^2}. \qquad \text{[III.16]}$$

The results are also listed in Table 2.

Table 2 presents an overview of calculated energies and nuclear radii of various $\bar{K}$ nuclear clusters at any input $\bar{K}N$ interaction strength. We can notice the following characteristics:

i) The binding energy increases with $|s_{\bar{K}N}^{(I=0)}|$. The degree of the increase is nearly the same for single-$\bar{K}$ clusters, whereas the degree of the binding energy increase for K^-K^-pp is almost twice as large as those of the single-$\bar{K}$ clusters. This large dependence of the K^-K^-pp energy on $|s_{\bar{K}N}^{(I=0)}|$ is understood from the different roles played by the most important poten-

Table 2.   Calculated $s_{\bar{K}N}^{(I=0)}$ dependences of the ground-state energies (E in MeV), the nucleon *rms* distributions for a point nucleon (R_{KNC}^{point} in fm), the nucleon *rms* distributions for a finite-sized nucleon (R_{KNC} in fm), *rms N-N* distances (R_{NN} in fm) and the effective densities ρ^{eff}/ρ_0 for K^-p, K^-K^-p, K^-pp, K^-ppn and K^-K^-pp. The values for the standard strength of the $\bar{K}N$ interaction ($s_{\bar{K}N}^{(I=0)} = -1.37$) are shown in gothic letters

	K^-p			K^-K^-p		
$s_{\bar{K}N}^{(I=0)}$	E	R_{KNC}^{point}	R_{KNC}	E	R_{KNC}^{point}	R_{KNC}
−1.2	−8.3	0.75	1.16	−9.1	1.59	1.82
−1.3	−18.0	0.55	1.04	−20.1	1.05	1.37
−1.37	**−26.6**	**0.47**	**1.00**	**−30.4**	**0.84**	**1.22**
−1.4	−30.7	0.44	0.98	−35.4	0.78	1.18
−1.5	−46.2	0.38	0.96	−54.8	0.63	1.08
−1.6	−64.2	0.34	0.94	−78.1	0.54	1.03
−1.7	−84.4	0.31	0.93	−105.1	0.47	1.00

	K^-pp					K^-ppn					K^-K^-pp				
$s_{\bar{K}N}^{(I=0)}$	E	R_{KNC}^{point}	R_{KNC}	R_{NN}	ρ^{eff}/ρ_0	E	R_{KNC}^{point}	R_{KNC}	R_{NN}	ρ^{eff}/ρ_0	E	R_{KNC}^{point}	R_{KNC}	R_{NN}	ρ^{eff}/ρ_0
−1.2	−23.8	1.06	1.38	1.93	1.48	−42	1.15	1.45	1.89	1.58	−43	0.91	1.27	1.57	2.75
−1.3	−39.0	0.94	1.29	1.73	2.06	−57	1.09	1.40	1.80	1.83	−70	0.82	1.20	1.43	3.64
−1.37	**−51.5**	**0.89**	**1.25**	**1.62**	**2.50**	**−69**	**1.06**	**1.37**	**1.75**	**1.99**	**−93**	**0.76**	**1.16**	**1.35**	**4.33**
−1.4	−57.3	0.86	1.23	1.58	2.70	−74	1.05	1.37	1.73	2.06	−104	0.74	1.15	1.31	4.73
−1.5	−78.3	0.81	1.19	1.48	3.28	−95	1.00	1.33	1.66	2.33	−144	0.69	1.12	1.22	5.86
−1.6	−101.9	0.76	1.16	1.40	3.88	−117	0.97	1.31	1.61	2.55	−190	0.66	1.10	1.09	8.22
−1.7	−127.9	0.72	1.14	1.32	4.63	−142	0.94	1.29	1.56	2.80	−241	0.63	1.08	0.94	12.8

tial energy, $V_{\bar{K}N}^{(I=0)}$, whose weight in the energy is 1 for $\bar{K}N$, 3/2 for $\bar{K}\bar{K}N$, $\bar{K}NN$ and $\bar{K}NNN$, and 3 for $\bar{K}\bar{K}NN$.

ii) The nuclear radii by nucleon distributions ($\bar{K}$ excluded) decrease with $|s_{\bar{K}N}^{(I=0)}|$, as initially predicted from the variational calculations of ref. 1. The nuclear shrinkage due to the attractive $\bar{K}N$ interaction is shown here as a general feature of $\bar{K}$ nuclear systems. The very much shrunk K^-K^-pp system is of particular importance. However, the behavior of the nuclear sizes with $|s_{\bar{K}N}^{(I=0)}|$ is different from that of the binding energies. The nuclear density seems to be saturated, where the binding energy still increases.

C. Higher-order effects of increased $\bar{K}N$ attractions. When the $\bar{K}N$ attraction is increased, the potential, kinetic and binding energies of kaonic nuclear clusters are drastically enlarged, as shown in Fig. 3(a) for K^-p, (b) for K^-pp and (c) for K^-K^-pp.

In the case of the K^-p system, (a), only a 15% increase of the K^-p interaction makes the binding energy of the system 2.24-times as large as that for the standard strength. Its reason can be understood as follows. At the standard strength, $s_{\bar{K}N}^{(I=0)}(\text{Std}) = -1.37$, the binding energy of the K^-p system, 26.6 MeV, is a result of large cancellation between the potential energy of −182.9 MeV and the kinetic

energy of 156.2 MeV. At the 15% strengthened $s_{\bar{K}N}^{(I=0)}$ interaction the potential energy of the system changes to −293.6 MeV with a 61% enhancement in the absolute value, where 46 (= 61 − 15)% comes from the higher-order effect of the increased $\bar{K}N$ attraction, which gives rise to a shrinkage of the wave function. This shrinkage also enhances the kinetic energy from 156.2 MeV to 233.9 MeV, partly cancelling the enhancement of the potential energy. In sum, the binding energy of K^-p increases more than double from 26.6 MeV to 59.7 MeV due to the 15% increase of the super-strong K^-p attractive interaction.

Similar enhancement behaviors are seen for K^-pp, (b) and for K^-K^-pp, (c). In the case of K^-pp the interaction between K^- and the pp core, which can be derived by a convolution procedure, becomes of longer range than the original K^-p interaction. Generally, the higher-order effect of long-range interaction becomes less effective so that in limit the potential energy of the system is well-estimated in a Born approximation. This long-range property of the K^-pp interaction explains that the enhancement factors in the K^-pp case are rather damp compared with those in the K^-p case. In the case of K^-K^-pp, where the number of K^-p interaction is multiplied, the enhancement factors again rapidly increase
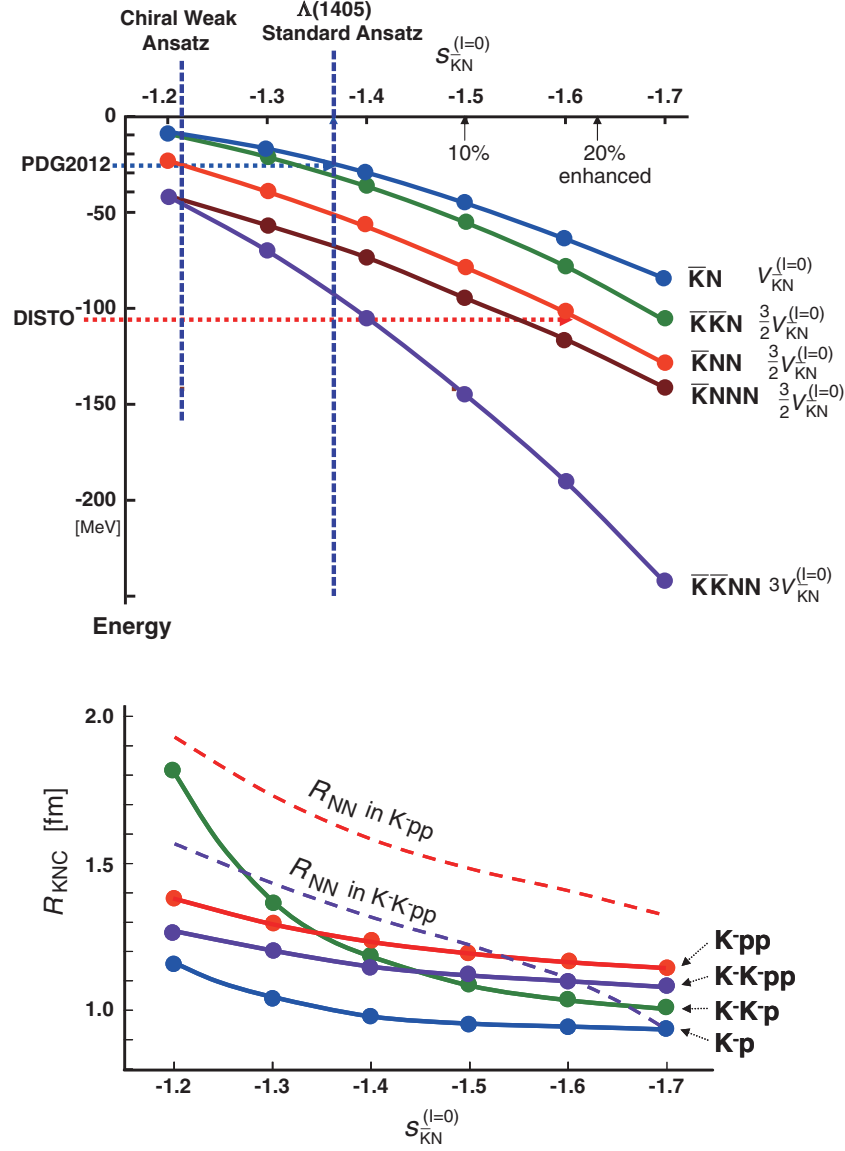
Fig. 2. Global view of the calculated bound-state energies (upper) and sizes (lower), R_{KNC} and R_{NN} of $\bar{K}$ nuclear clusters as functions of the $\bar{K}N$ interaction strength, $s_{\bar{K}N}^{(I=0)}$. The zones of the standard "$\Lambda(1405)$ ansatz" and the "Chiral" ansatz are shown by vertical broken lines. The experimental value of the mass of $K^- pp$ as observed by DISTO[13] is shown by a horizontal broken line, where a relativistic correction for the binding energy around $10\,\mathrm{MeV}$ is not taken into account.

toward quite a large binding as seen in Fig. 3(c). Experimental information is awaited especially for highly compact system, $K^- K^- pp$.

D. Density distributions of $\bar{K}$ nuclear clusters. To investigate the feature of these large bindings and compact sizes, we analyzed the wave functions obtained in the present calculation. We show here some remarkable consequences.

1. N-density distributions. Figure 4 (left) shows the nucleon density distributions, $\rho_N(r)$, where r is the distance of the nucleon from the center of mass of (a) $K^- pp$, (b) $K^- ppn$ and (c) $K^- K^- pp$ for various values of $s_{\bar{K}N}^{(I=0)} = -1.2, -1.3, -1.4, -1.5, -1.6$ and -1.7. The nucleon density distribution in $K^- pp$ has a depression near the center of mass, which arises from the repulsive interaction between two nucleons at short NN distances. We note that this depression disappears by kinematical reason when another N ($K^- ppn$) or $\bar{K}$ ($K^- K^- pp$) is added to the $\bar{K}NN$ system.
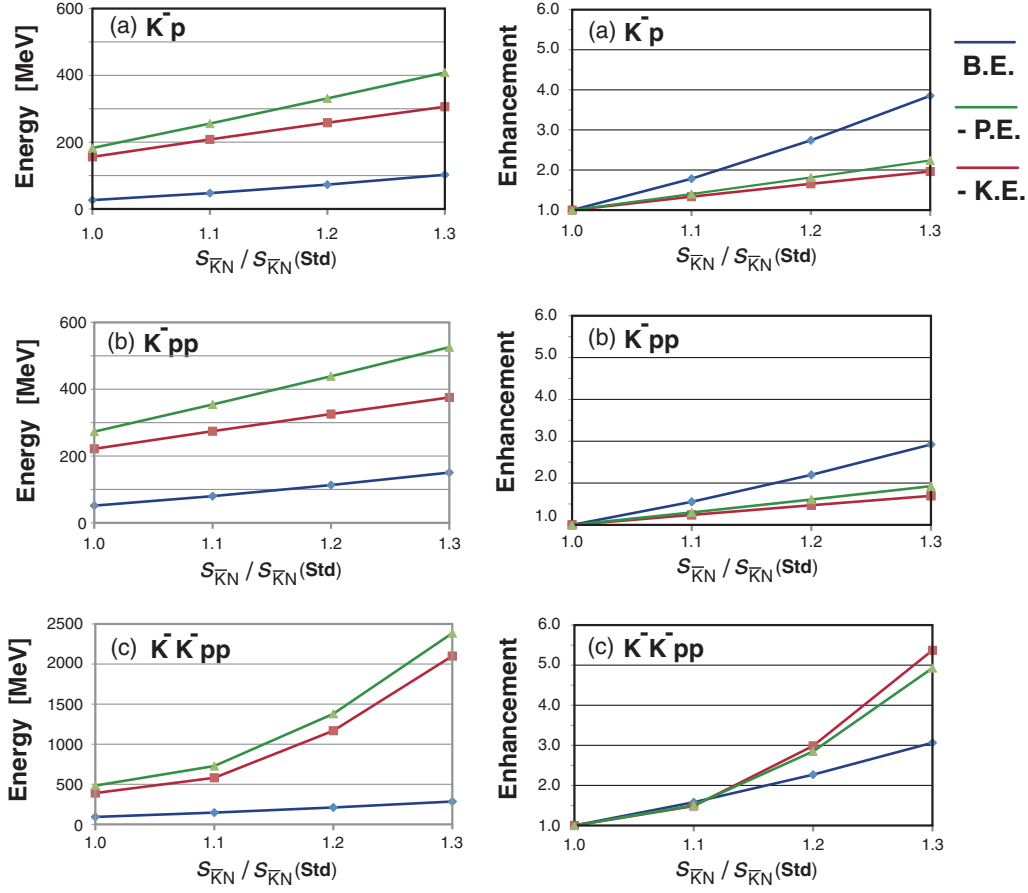
Fig. 3. Illustration of the energy values of binding (B.E.), potential (P.E.) and kinetic (K.E.) energies (left) and their enhancements (right) as functions of the interaction strength $f = s_{\bar{K}N}^{(I=0)}/s_{\bar{K}N}^{(I=0)}$(Std), indicating enormous higher-order effects of wave function shrinkage caused by the increase of $\bar{K}N$ attraction.

Figure 4 (right) shows the same distributions but multiplied by r^2 ($r^2\rho_N(r)$). From these we can see that, when the $\bar{K}N$ attraction is strengthened, strong shrinkage occurs due to an increase of the maxima at around $r = 0.5$ fm and their inward shifts. Especially, the trend of the increase of the maxima in K^-K^-pp is significant. Besides, from the figure on the left bottom, we can see a growth of the inner amplitude ($r < 0.2$ fm); it remains small for $s_{\bar{K}N}^{(I=0)} = -1.2, -1.3,$ -1.4 and -1.5, but then, it drastically increases for $s_{\bar{K}N}^{(I=0)} = -1.6$ and -1.7, both in amplitude and in size of this region, showing a growth of a nuclear high-density region in the center of this double-$\bar{K}$ nuclear system.

2. NN distance distributions and effective density.
Figure 5 (left) shows the probability density distributions of the N-N distance $\rho_{NN}(r)$ in (a) K^-pp (b) K^-ppn and (c) K^-K^-pp for $s_{\bar{K}N}^{(I=0)} = -1.2, -1.3, -1.4,$ $-1.5, -1.6,$ and -1.7, where r is the N-N distance.

We can see that in K^-pp and K^-ppn $\rho_{NN}(r)$ has a nodal behavior at around $r = 0.2$ fm, and has an inner amplitude at $r < 0.2$ fm. This nodal behavior arises from the rank-2 nature of the NN potential. In K^-K^-pp, this inner amplitude becomes significantly enhanced. The three figures on the right of Fig. 5 show the same distribution, but multiplied by r^2, $r^2\rho_{NN}(r)$, which is normalized as $\int_0^\infty dr\, r^2\rho_{NN}(r) = 1$. From these figures, we can see that while the inner amplitude remains small when the $\bar{K}N$ interaction is strengthened in K^-pp and K^-ppn, it becomes much enhanced, and the size of this region also increases (up to around $r = 0.5$ fm for $s_{\bar{K}N}^{(I=0)} = -1.6$ and -1.7) in K^-K^-pp. This indicates the fact that addition of one anti-kaon to K^-pp leads to a situation in which two nucleons can get very close to each other in spite of the strong inner repulsion of the NN interaction.

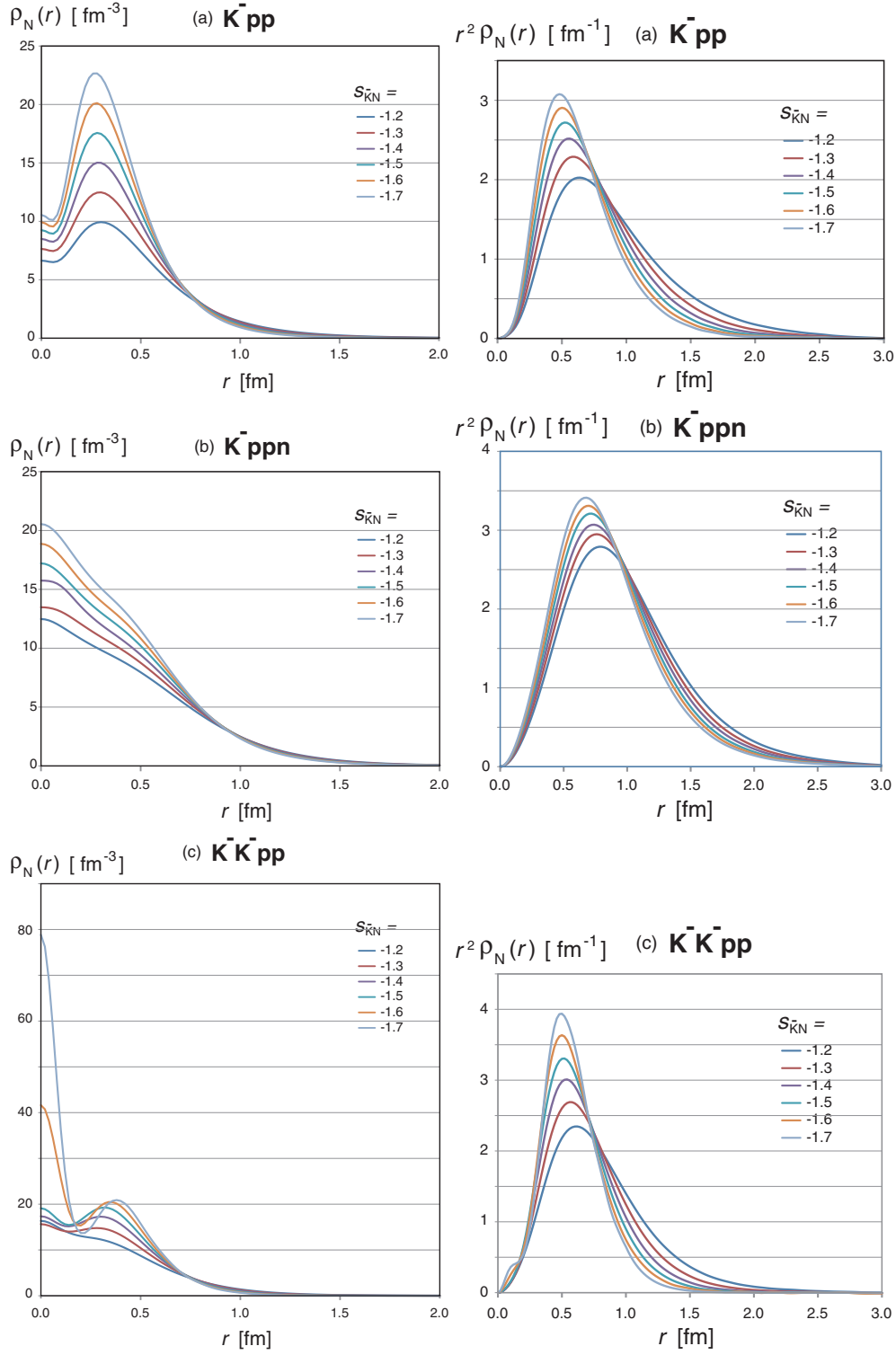The $^1S_0$ NN potential of Ikeda and Sato,[39] which we employed in our K^-K^-pp calculation, reproduces

Fig. 4.   Nucleon density distributions, (left) $\rho_N(r)$ and (right) $r^2\rho_N(r)$, with respect to the center of mass for (a) K^-pp, (b) K^-ppn and (c) K^-K^-pp for various values of $s_{\bar{K}N}^{(I=0)} = -1.2, -1.3, -1.4, -1.5, -1.6$ and -1.7. They are normalized so that $\int_0^\infty r^2 dr \rho(r) =$ number of the nucleons. No nucleon size is included.

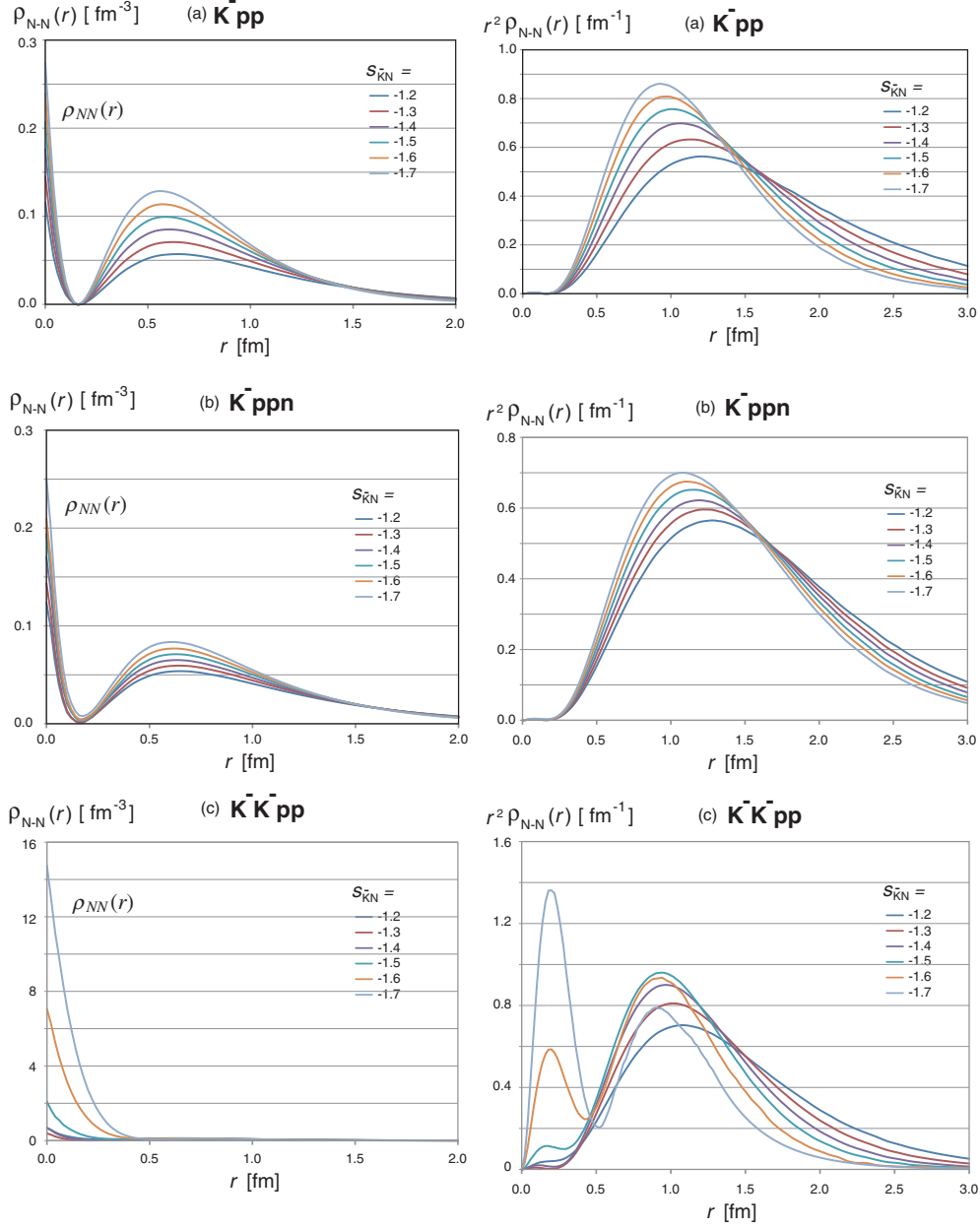Fig. 5. NN distance distributions (left) $\rho_{N-N}(r)$ and (right) $r^2\rho_{N-N}(r)$ in (a) K^-pp, (b) K^-ppn and (c) K^-K^-pp for $s_{\bar{K}N}^{(I=0)} = -1.2, -1.3,$ $-1.4, -1.5, -1.6,$ and -1.7. No nucleon size is included. As the absolute value of $s_{\bar{K}N}^{(I=0)}$ becomes larger, the distribution in the tail region becomes relatively more pulled inward.

the experimental $^1S_0$ phase shift up to $E_{lab} =$ 300 MeV. This means that the NN interaction is probed up to around $r = 0.5$ fm by this potential model. Though the validity of this NN potential for $r < 0.5$ fm is not supported, it can be a general argument that the relative motion of two nucleons in the point nucleon model has a non-zero amplitude at $r < 0.5$ fm. The present calculation shows that,

if there is non-zero amplitude at $r < 0.5$ fm, even if it is small, the inner amplitude can grow by coupling to the short-ranged $\bar{K}N$ attraction. If there are two anti-kaons present, the two-fold attraction mechanism leads to a significant growth of this inner amplitude in magnitude and in range, when the $\bar{K}N$ interaction is strengthened.
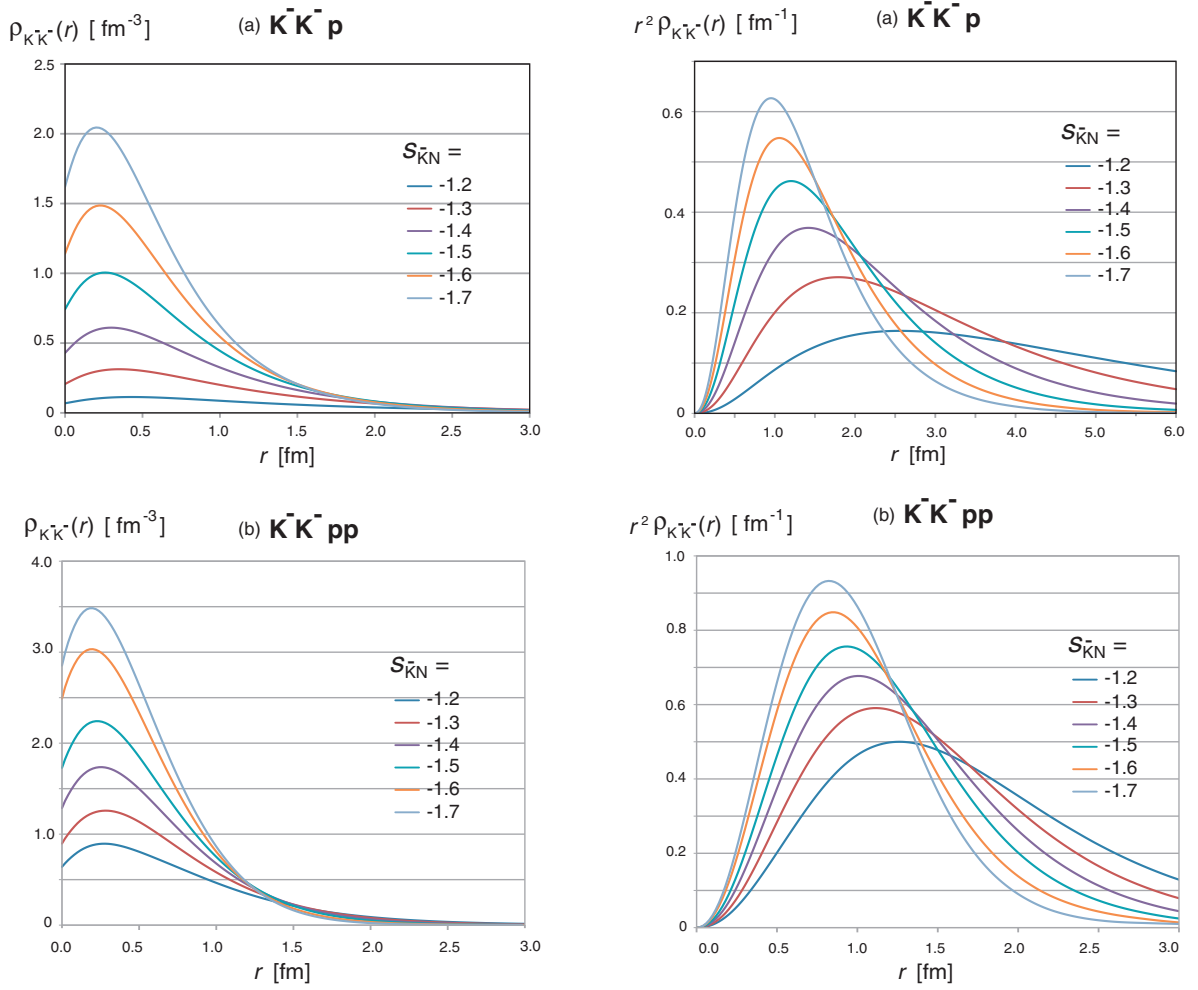
Fig. 6.   Probability distribution of the $\bar{K}\bar{K}$ distance (left) $\rho_{K^-K^-}(r)$ and (right) $r^2\rho_{K^-K^-}(r)$ in (upper) K^-K^-p and (lower) K^-K^-pp.

We calculated the mean N-N distances for K^-pp, K^-ppn and K^-K^-pp,

$$R_{NN} = \sqrt{\int_0^\infty r^4\rho_{NN}(r)\mathrm{d}r}, \qquad \text{[III.17]}$$

for various values of $s_{\bar{K}N}^{(I=0)}$, as shown in Table 2. Using the known NN distance,[6),56)]

$$R_{NN}^{(\mathrm{ord})} = 2.2\,\mathrm{fm}, \qquad \text{[III.18]}$$

for the ordinary nuclear density of $\rho_0 = 0.17\,\mathrm{fm}^{-3}$, we could calculate the ratio, which can be called the "effective nuclear density" of KNC, as follows:

$$\rho^{(\mathrm{eff})} = \left[\frac{R_{NN}^{(\mathrm{ord})}}{R_{NN}}\right]^3 \rho_0. \qquad \text{[III.19]}$$

These values are presented in Table 2. For instance, $\rho^{(\mathrm{eff})} = 2.5\rho_0$ in K^-pp, and $\rho^{(\mathrm{eff})} = 4.3\rho_0$ in K^-K^-pp at

the standard $\bar{K}N$ interaction. The $\rho^{(\mathrm{eff})}$ increases with $|s_{\bar{K}N}^{(I=0)}|$.

3. $\bar{K}$-$\bar{K}$ distance distributions. To investigate the effect of the repulsion between two $\bar{K}$'s, we show in Fig. 6 the probability density distribution of the $\bar{K}\bar{K}$ distance $\rho_{K^-K^-}(r)$ (left) and $r^2\rho_{K^-K^-}(r)$ (right) in K^-K^-p (upper) and K^-K^-pp (lower). We note that the $\bar{K}\bar{K}N$ system has an appreciable amplitude for those configurations where the two anti-kaons are very near to each other, already for lower values of $|s_{\bar{K}N}^{(I=0)}|$. By the addition of one nucleon, this inner amplitude grows significantly, and the two $\bar{K}$'s become much closer to each other. Further, the inner amplitude increases drastically when $|s_{\bar{K}N}^{(I=0)}|$ is increased. These features strongly indicate that the effect of the repulsion between the two anti-kaons against the bindings of the $\bar{K}$ nuclear systems is
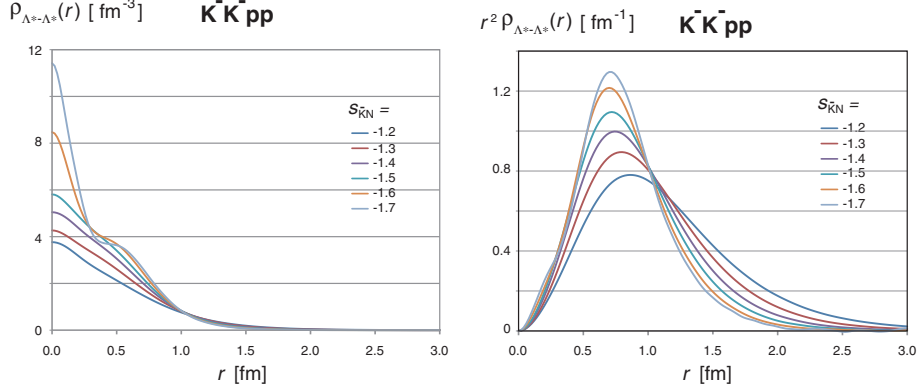
Fig. 7. Probability distribution of the distance between the centers of mass of two Λ^* clusters in $K^- K^- pp$, when $s_{\bar{K}N}^{(I=0)}$ is varied from -1.2 to -1.7.

not important. This is against the prevailing belief that because of the $\bar{K}$-$\bar{K}$ repulsion no formation of dense $\bar{K}$ nuclear matter is possible, but is consistent with a dynamical mechanism for reducing the $\bar{K}$-$\bar{K}$ repulsion due to the $\bar{K}N$ formation.[19),20)]

4. Λ^*-Λ^* distance distributions in $\bar{K}\bar{K}NN$. Because one K^- and one proton form a compact system (Λ^*), $K^- K^- pp$ is an important system to study the relative motion of two Λ^* particles. Figure 7 shows the probability density distribution of the distance between the centers of mass of two Λ^* clusters in $K^- K^- pp$, when $s_{\bar{K}N}^{(I=0)}$ is varied from -1.2 to -1.7. It is interesting that as the attraction between K^- and p becomes stronger, the maximum of the distribution seems to converge to a distance of around 0.7 fm. In addition, there seems to grow an inner bump in the distribution at $r \leq 0.3$ fm, particularly for $s_{\bar{K}N}^{(I=0)} = -1.6$ and -1.7. Combined with the strongly enhanced NN inner amplitude for these $s_{\bar{K}N}^{(I=0)}$ values, this indicates the possibility of the growth of a very high-density configuration in the center of this double K^- nucleus, where all of the two $\bar{K}$'s and two protons become very near to each other.

IV. Relativistic effect on $\bar{K}$ binding

The calculations so far made are based on a non-relativistic (NR) treatment of few-body systems. For the very deeply bound $\bar{K}$, however, relativistic corrections are indispensable.[57)] The relativistic effect can be taken into account by using the Klein-Gordon (KG) equation for K^-,

$$\left\{ -\frac{\hbar^2}{2m_K}\vec{\nabla}^2 + U^{\mathrm{opt}} \right\}|\Phi\rangle = \left(\varepsilon_{\mathrm{KG}} + \frac{\varepsilon_{\mathrm{KG}}^2}{2m_K c^2} \right)|\Phi\rangle,$$

$$U^{\mathrm{opt}} = U_{\mathrm{s}} + U_{\mathrm{v}} + \frac{U_{\mathrm{s}}^2 - U_{\mathrm{v}}^2 + \varepsilon_{\mathrm{KG}}U_{\mathrm{v}}}{2m_K c^2}, \qquad [\text{IV.20}]$$

where $\varepsilon_{\mathrm{KG}}$ is the rest-mass-subtracted energy of K^-, and U_{s} (U_{v}) is a scalar (vector) mean-field potential for K^- from the *shrunk nuclear core*. Detailed realistic calculations of U^{opt} are in progress.

If we obtain from few-body NR calculations the lowest energy, ε_{S}, of the Schrödinger equation with the same optical potential, U^{opt},

$$\left\{ -\frac{\hbar^2}{2m_K}\vec{\nabla}^2 + U^{\mathrm{opt}} \right\}|\Phi\rangle = \varepsilon_{\mathrm{S}}|\Phi\rangle, \qquad [\text{IV.21}]$$

the KG energy is calculated by the relation,

$$\varepsilon_{\mathrm{KG}} = m_K c^2 \left(\sqrt{1 + \frac{2\varepsilon_{\mathrm{S}}}{m_K c^2}} - 1 \right). \qquad [\text{IV.22}]$$

Obviously, this relation means that, when the NR energy, ε_{S}, drops down to $-m_K c^2/2$, the relativistic energy, $\varepsilon_{\mathrm{KG}}$, becomes $-m_K c^2$, namely, the total mass of K^- becomes zero ("kaon condensation regime"), as shown in Fig. 8. This relativistic effect would become particularly large in the case of $K^- K^- pp$, where the core nucleus is strongly shrunk with a highly excited internal energy and, therefore, $|\varepsilon_{\mathrm{S}}|$ is much bigger than the value naively estimated from $B(K^- K^- pp)$ denoted in Fig. 2.

Roughly speaking, the relativistic correction for $\varepsilon_{\mathrm{S}} \sim 100$ MeV is: $\Delta\varepsilon_{\mathrm{KG}} = \varepsilon_{\mathrm{KG}} - \varepsilon_{\mathrm{S}} \approx -10$ MeV. The relativistic correction for $K^- K^- pp$ becomes very large, when the chiral symmetry restoration effect is taken into account.

V. Effect of chiral symmetry restoration in $\bar{K}$ nuclear systems

The binding energy of $K^- pp$, $B_K = 103$ MeV, as observed in the DISTO experiment,[13)] turned out to be much larger than the original predicted value (48 MeV,[2)] 51.5 MeV in the present work) based on
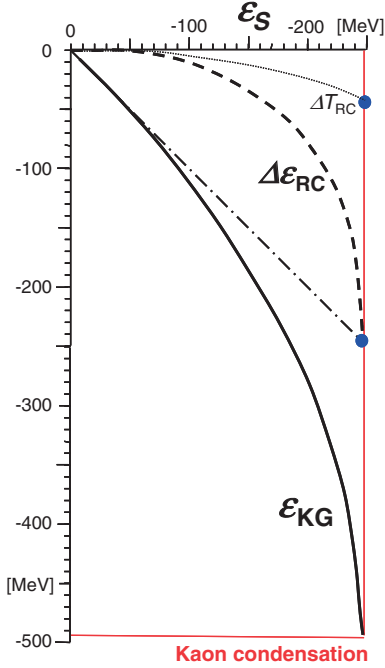
Fig. 8.   Comparison between the Klein-Gordon energy, $\varepsilon_{\mathrm{KG}}$, and the Schrödinger energy, ε_{S}. The relativistic correction, $\Delta\varepsilon_{\mathrm{RC}} = \varepsilon_{\mathrm{KG}} - \varepsilon_{\mathrm{S}}$, is shown by a broken curve. As $\varepsilon_{\mathrm{S}} \to -m_K c^2/2$, $\varepsilon_{\mathrm{KG}}$ becomes $-m_K c^2$ (Kaon condensation).

the standard $\Lambda(1405)$ ansatz. This infers that the $I = 0$ $\bar{K}N$ interaction is effectively enhanced by about 25% for some reasons.[7] We examined the problem of the interaction ranges in the adopted NN and $\bar{K}N$ interactions, and found that possible changes of the ranges that are consistent with the mass and width of $\Lambda(1405)$ cannot account for the large binding energy. Thus, the present standard value of the $\bar{K}N$ interaction that corresponds to $B_K = 27\,\mathrm{MeV}$ of $\Lambda(1405)$ is rather robust; it cannot be increased by 25%. It is thus plausible to investigate the problem as to "how the $\bar{K}N$ interaction changes in the nuclear medium". The relativistic correction in KNC is substantial as we have seen in the preceding Section IV, but for $B_K = 103\,\mathrm{MeV}$, it is about 10% effect, and thus it is not the main cause.

We now consider possible in-medium effects on chiral-symmetry breaking and restoration that occur spontaneously in the meson-nucleon interactions.[58] Both the T-matrices of the s-wave πN and $\bar{K}N$ interactions of Nambu-Goldstone bosons are expressed in relation to the pion and kaon decay constants, f_π and f_K, respectively, through the Weinberg–Tomozawa theorem,[59),60]

$$T_{\pi N}^{(I=3/2)} = \frac{\omega_\pi}{f_\pi^2}, \qquad [\text{V.23}]$$

$$T_{\bar{K}N}^{(I=0)} = -\frac{\omega_K}{f_K^2}, \qquad [\text{V.24}]$$

where the T matrices are inversely proportional to f_π^2 and f_K^2. They are further related to the current quark masses, (m_u, m_d, m_s), and quark condensates in the QCD vacuum, according to the Gell-Mann–Oakes–Renner (GOR) relation,[61]

$$m_\pi^2 f_\pi^2 = -4m_q\langle 0|\bar{q}q|0\rangle, \qquad [\text{V.25}]$$

$$m_K^2 f_K^2 = -(m_q + m_s) \\ \times [\langle 0|\bar{q}q|0\rangle + \langle 0|\bar{s}s|0\rangle], \qquad [\text{V.26}]$$

where $m_q = (m_u + m_d)/2$, and $\langle 0|\bar{q}q|0\rangle = \langle 0|(\bar{u}u + \bar{d}d)/2|0\rangle$ is a (u,d) quark condensate in free space. The quark condensate is the order parameter of the QCD vacuum,[58] and they are subject to changes in the nuclear medium[62)–65] as $\langle 0|\bar{q}q|0\rangle_{\mathrm{free}} \to \langle 0|\bar{q}q|0\rangle_\rho$ in the case of πN and $[\langle 0|\bar{q}q|0\rangle_{\mathrm{free}} + \langle 0|\bar{s}s|0\rangle_{\mathrm{free}}] \to [\langle 0|\bar{q}q|0\rangle_\rho + \langle 0|\bar{s}s|0\rangle_\rho]$ in the case of $\bar{K}N$. Our concern is only on the qualitative change of the T matrices, and we expect the following enhancement factors at a nuclear density of ρ. For the case of πN, the ratio of the s-wave isovector interaction with a potential parameter b_1 is given by

$$F_{\pi N}(\rho) = \frac{b_1^\rho}{b_1^{\mathrm{free}}} = \frac{|\langle 0|\bar{q}q|0\rangle_{\mathrm{free}}|}{|\langle 0|\bar{q}q|0\rangle_\rho|} \approx \frac{1}{1-\alpha\rho}, \quad [\text{V.27}]$$

with α as a parameter. Such an enhancement was observed in deeply bound pionic states,[30)–32] where the parameter α was deduced to be $(0.36 \pm 0.08) \times \rho_0^{-1}$ with $\rho_0 = 0.17\,\mathrm{fm}^{-3}$ being the normal nuclear density. This value is in good agreement with theoretical predictions.[66]

In the $\bar{K}N$ sector the enhancement of the $\bar{K}N$ interaction is given by

$$F_{\bar{K}N}(\rho) = \frac{T_{\bar{K}N}^\rho}{T_{\bar{K}N}^{\mathrm{free}}} = \frac{|\langle 0|\bar{q}q|0\rangle_{\mathrm{free}} + \langle 0|\bar{s}s|0\rangle_{\mathrm{free}}|}{|\langle 0|\bar{q}q|0\rangle_\rho + \langle 0|\bar{s}s|0\rangle_\rho|}, \quad [\text{V.28}]$$

where the $\langle 0|\bar{s}s|0\rangle_{\mathrm{free}}$ is known to be around $0.8\langle 0|\bar{q}q|0\rangle_{\mathrm{free}}$.[67] A similar decrease of the quark condensates, thus, increase of the attractive $\bar{K}N$ interaction, is expected. Here, we can foresee that its effect should be much more spectacular compared with the πN case, since the strongly attractive $\bar{K}N$ interaction tends to induce tremendous higher-order effects, in contrast to the case of the πN interaction of repulsive character. The most important effect in the $\bar{K}N$ case is substantial nuclear shrinkage caused by the strongly attractive force, as we have considered in the preceding section. So far, no such effect has

been taken into account in terms of the modification of the $\bar{K}N$ interaction.

In the present note we attempt to understand this effect qualitatively by applying the concept of "clearing of QCD vacuum" introduced by Brown, Kubodera and Rho.[68] This model states that the QCD vacuum expressed by the quark condensate is reduced by the amount of clearing of the QCD vacuum by the presence of nucleons. We extend the BKR model to $\bar{K}$ nuclear bound systems (with a nucleon number n), postulating the following enhancement factors for the πN and $\bar{K}N$ cases, respectively:

$$F_{\pi N} = \frac{|\langle 0|\bar{q}q|0\rangle_0|}{|\langle 0|\bar{q}q|0\rangle_\rho|} \approx \frac{1}{1 - \Omega}, \qquad [\text{V.29}]$$

$$F_{\bar{K}N} = \frac{|\langle 0|\bar{q}q|0\rangle_0|}{|\langle 0|\bar{q}q|0\rangle_\rho|} \approx \frac{1}{1 - 0.5\,\Omega} \qquad [\text{V.30}]$$

with a "QCD vacuum clearing" factor of Ω, which is given by the ratio of the volume of the nucleon (v_N) that clears the QCD vacuum to the nuclear volume (V_{nucl}) as

$$\Omega = \frac{n \cdot v_N}{V_{\text{nucl}}}. \qquad [\text{V.31}]$$

We take an "*rms* volume" for v_N,

$$v_N = \frac{4\pi}{3} r_N^3 = 2.85 \ [\text{fm}^3], \qquad [\text{V.32}]$$

corresponding to an *rms* nucleon radius of $r_N = 0.88\,\text{fm}$,[24] since it represents a dense region of the nucleon that is expected to clear the volume of the QCD vacuum. In the case of the $\bar{K}N$ case, the denominator in eq. [V.30] is approximated to $1 - 0.5\,\Omega$, since the chiral restoration effect dominates the $\langle 0|\bar{q}q|0\rangle$ term in eq. [V.28], so that $\langle 0|\bar{s}s|0\rangle_\rho$ is close to $\langle 0|\bar{s}s|0\rangle_{\text{free}}$.[63]

In the case of a normal nucleus having a mass number A and a nuclear radius of $R_A = 1.2 \times A^{1/3}$ fm at the standard nuclear density $\rho_0 = 0.17\,\text{fm}^{-3}$, the nuclear volume is

$$V_{\text{nucl}} = 7.24 \times A \ [\text{fm}^3]. \qquad [\text{V.33}]$$

Thus,

$$\Omega \approx 0.34\frac{\rho}{\rho_0}, \qquad [\text{V.34}]$$

which gives good agreement with the observation of $F_{\pi N}(\rho)$ in the deeply bound pionic case, eq. [V.27].

In the case of $\bar{K}$ clusters, how to define V_{nucl} is not obvious. Since few-body $\bar{K}N$ clusters do not provide a homogeneous medium, we evaluated V_{nucl} from V_{KNC} using the realistic wave functions.

Figure 9 shows the nucleon distributions $\rho_N(r)$ and $4\pi r^2 \rho_N(r)$ for $K^- pp$ and $K^- K^- pp$ both for point and finite-size nucleons in a schematical figure. We can define an effective radius, R_{eff}, for "80% volume" as

$$\int_0^{R_{\text{eff}}} r^2 \rho_N^{\text{finite}}(r)\mathrm{d}r = n \times 0.80. \qquad [\text{V.35}]$$

The effective nuclear volume is

$$V_{\text{eff}} = \frac{4\pi}{3} R_{\text{eff}}^3, \qquad [\text{V.36}]$$

which yields $\Omega_{\bar{K}N} = n \cdot v_N/V_{\text{eff}}$, as shown in Table 3. Using these values we can obtain enhancement factors for the $\bar{K}N$ interactions, $F_{\bar{K}N}$, which lead to enhanced interaction strengths, $s_{\bar{K}N}^{(1st)}$, with the same non-dimensional unit as $s_{\bar{K}N}$, where the suffix $(1st)$ means the first iteration of such renormalization.

Let us take $K^- pp$ as an example. As the first step, we take $s_{\bar{K}N}^{(I=0)} = -1.37$ so as to be consistent with the assumed binding energy of 27 MeV of $K^- p$ identified as $\Lambda(1405)$. The BKR procedure gives a renormalized interaction parameter, enhanced by a factor of 1.24. This in turn gives a renormalized interaction strength: $s_{\bar{K}N}^{(I=0)} = -1.37 \times 1.24 = -1.69$. It is known that the experimental binding energy of $K^- pp$, 103 MeV, obtained from the DISTO experiment,[13] is about a factor of 2 larger than the original few-body predictions taking into account the NN repulsion appropriately, 53 MeV,[2] 55–70 MeV,[37] 76 MeV,[39] and 51.5 MeV (present). This discrepancy, as shown in Fig. 2, can now be explained by an increase of the $\bar{K}N$ interactions due to chiral symmetry restoration.

Unfortunately, there is only one empirical data that we can take into account with confidence. We look forward to more experimental data to be produced in the near future.

VI. Concluding remarks

We have made a comprehensive systematic study for the kaonic nuclear systems $K^- p$, $K^- K^- p$, $K^- pp$, $K^- ppn$ and $K^- K^- pp$ by employing separable potential models for the NN, $\bar{K}N$ and $\bar{K}\bar{K}$ interactions. Our calculations based on the PDG interpretation of $\Lambda(1405)$ show deep bindings of $K^- pp$, $K^- ppn$ and $K^- K^- pp$ in contrast to the weak binding results based on the chiral SU(3) dynamics model of the $\bar{K}N$ interaction.

To globally view the deep nuclear binding and strong shrinkage induced by the short-ranged strong $\bar{K}N$ interaction, we created a reference diagram of the binding enegies of these kaonic nuclear systems
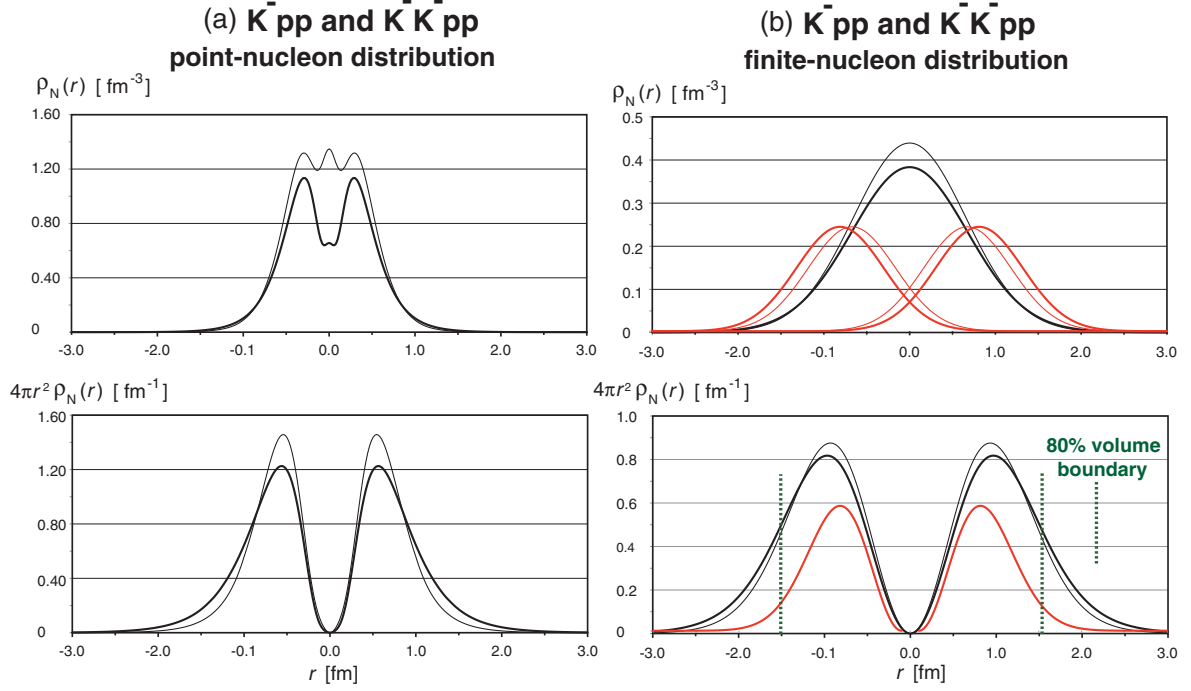
Fig. 9. Nucleon density distributions in K^-pp (solid curves) and K^-K^-pp (thin curves) at $s_{\bar{K}N}^{(I=0)}(\mathrm{Std}) = -1.37$, a) for a point nucleon and b) for a finite nucleon, (upper) $\rho_N(r)$ and (lower) $4\pi r^2\rho_N(r)$. The red curves represent the proton finite distributions when the two protons are located at the mean separation distances, R_{NN}.

Table 3. Effect of chiral symmetry restoration in K^-pp, K^-ppn and K^-K^-pp. R_{eff} is the radius corresponding to 80% volume of each KNC: V_{eff} [fm^3]. $\Omega_{\bar{K}N}$ = QCD-vacuum clearing factor. $F_{\bar{K}N}$ = enhancement factor of the $\bar{K}N$ interaction. $s_{\bar{K}N}^{(1\mathrm{st})}$ = renormalized interaction strength after the 1st iteration

	K^-pp					K^-ppn					K^-K^-pp				
$s_{\bar{K}N}$	R_{eff}	V_{eff}	$\Omega_{\bar{K}N}$	$F_{\bar{K}N}$	$s_{\bar{K}N}^{(1\mathrm{st})}$	R_{eff}	V_{eff}	$\Omega_{\bar{K}N}$	$F_{\bar{K}N}$	$s_{\bar{K}N}^{(1\mathrm{st})}$	R_{eff}	V_{eff}	$\Omega_{\bar{K}N}$	$F_{\bar{K}N}$	$s_{\bar{K}N}^{(1\mathrm{st})}$
-1.2	1.68	19.8	0.29	1.17	-1.40	1.77	23.1	0.37	1.23	-1.47	1.55	15.6	0.37	1.22	-1.47
-1.3	1.58	16.5	0.35	1.21	-1.57	1.71	21.0	0.41	1.26	-1.63	1.47	13.4	0.43	1.27	-1.65
$\mathbf{-1.37}$	**1.53**	**15.0**	**0.38**	**1.24**	$\mathbf{-1.69}$	**1.68**	**19.9**	**0.43**	**1.27**	$\mathbf{-1.75}$	**1.43**	**12.3**	**0.46**	**1.30**	$\mathbf{-1.78}$
-1.4	1.51	14.5	0.39	1.25	-1.74	1.67	19.6	0.44	1.28	-1.79	1.42	11.9	0.48	1.31	-1.84
-1.5	1.46	13.1	0.43	1.28	-1.92	1.63	18.3	0.47	1.31	-1.96	1.38	11.0	0.52	1.35	-2.02
-1.6	1.43	12.2	0.47	1.31	-2.09	1.61	17.4	0.49	1.33	-2.12	1.35	10.4	0.55	1.38	-2.21
-1.7	1.40	11.4	0.50	1.33	-2.26	1.58	16.6	0.52	1.35	-2.29	1.34	10.0	0.57	1.40	-2.38

with respect to the strength of the $\bar{K}N$ attraction, and calculated the probability density distributions of the nucleons and the relative distance of the two nucleons from the obtained wave function. Besides the increase in binding energies with the increase in the $\bar{K}N$ attraction, there appears to be a considerable shrinkage behavior of the size of the nucleonic motion in these $\bar{K}$ nuclear systems, as can be seen from Fig 4. A main shrinkage occurs by inward shifts of the maxima in $r^2\rho(r)$ at around $0.5\,\mathrm{fm}$ and of the tail parts ($r > 1\,\mathrm{fm}$).

Especially, we can see a notable shrinkage in K^-K^-pp, where the "super-strong nuclear force" mediated by an anti-kaon between two nucleons[6),7)] works twofold, in a simple counting, compared with K^-pp. The repulsive force between the two anti-kaons is not effective to prevent this double attraction mechanism (see also refs. 19), 20)). Surprisingly, as shown in Fig. 5(c), the NN relative wave function reveals an appreciable inner amplitude at very short NN distances ($r_{NN} < 0.5\,\mathrm{fm}$, inside of the size of the nucleons themselves), whereas K^-pp and

K^-ppn show only small amplitudes (Fig. 5(a,b)). Our calculation indicates that this inner amplitude in the K^-K^-pp system grows appreciably when we take around $s_{KN}^{(I=0)} = -1.5$ or stronger values. This behavior of the enhanced NN inner amplitudes suggests that the short-ranged attraction due to the exchange of ρ meson, which is taken into account in the range of our $\bar{K}N$ interaction as the underlying process of the Weinberg–Tomozawa term, sensitively couples to the two nucleons when located almost next to each other, thus generating the growth of extremely high-density nuclear configurations in the central region of the $\bar{K}\bar{K}$ nuclear systems.

　　In analyzing the DISTO experiment, a compact K^-pp state is obtained, the binding energy of which is much deeper than the original theoretical predictions. To clarify this situation, we conducted an analysis on the effect of the partial restoration of chiral symmetry on the $\bar{K}N$ interaction on the basis of the "clearing QCD vacuum" model of Brown, Kubodera and Rho.[68] In this analysis, we calculated the QCD vacuum clearing factor, Ω, from the obtained nucleon density distributions. Our analysis shows that the compact K^-pp state indicated from the DISTO experiment is consistent with the strengthening of the $\bar{K}N$ interaction due to the partial restoration of the chiral symmetry. Our analysis further suggests an even stronger $\bar{K}N$ interaction in the K^-K^-pp system, *i.e.*, a very compact K^-K^-pp state. This could thus be a possible mechanism to generate extremely high density, and requires further theoretical studies. For a systematic understanding of the chiral symmetry restoration in dense nuclear matter, we strongly encourage efforts to conduct experimental searches for kaonic nuclear bound systems including K^-K^-pp, in addition to K^-pp.[69]–[72]

Acknowledgments

References

1) Akaishi, Y. and Yamazaki, T. (2002) Nuclear $\bar{K}$ bound states in light nuclei. Phys. Rev. C Nucl. Phys. **65**, 044005.

2) Yamazaki, T. and Akaishi, Y. (2002) (K^-, π^-) production of nuclear $\bar{K}$ bound states in proton-rich systems via Λ^* doorways. Phys. Lett. B **535**, 70–76.

3) Doté, A., Horiuchi, H., Akaishi, Y. and Yamazaki, T. (2004) High-density $\bar{K}$ nuclear systems with isovector deformation. Phys. Lett. B **590**, 51–56.

4) Doté, A., Horiuchi, H., Akaishi, Y. and Yamazaki, T. (2004) Kaonic nuclei studied based on a new framework of antisymmetrized molecular dynamics. Phys. Rev. C Nucl. Phys. **70**, 044313.

5) Yamazaki, T., Doté, A. and Akaishi, Y. (2004) Invariant-mass spectroscopy for condensed single- and double-$\bar{K}$ nuclear clusters to be formed as residues in relativistic heavy-ion collisions. Phys. Lett. B **587**, 167–174.

6) Yamazaki, T. and Akaishi, Y. (2007) Super strong nuclear force caused by migrating $\bar{K}$ mesons— Revival of the Heitler-London-Heisenberg scheme in kaonic nuclear clusters. Proc. Jpn. Acad., Ser. B **83**, 144–150.

7) Yamazaki, T. and Akaishi, Y. (2007) Basic $\bar{K}$ nuclear cluster, K^-pp, and its enhanced formation in the $p + p \rightarrow K^+ + X$ reaction. Phys. Rev. C Nucl. Phys. **76**, 045201.

8) Heitler, W. and London, F. (1927) Wechselwirkung neutraler Atome und homoopolare Bindung nach der Quantenmechanik. Z. Phys. **44**, 455–472.

9) Nishijima, K. (2008) cover page and caption of Proc. Jpn. Acad., Ser. B **84**, issue 7.

10) Maggiora, M. *et al.* (2001) New results from DISTO for spin observables in exclusive hyperon production. Nucl. Phys. A **691**, 329c–335c.

11) Zychor, I. *et al.* (2008) Lineshape of the $\Lambda(1405)$ hyperon measured through its $\Sigma^0\pi^0$ decay. Phys. Lett. B **660**, 167–171.

12) Cho, S. *et al.* (2011) Identifying multiquark hadrons from heavy ion collisions. Phys. Rev. Lett. **106**, 212001.

13) Yamazaki, T. *et al.* (2010) Indication of a deeply bound and compact K^-pp state formed in the $pp \rightarrow p\Lambda K^+$ reaction at 2.85 GeV. Phys. Rev. Lett. **104**, 132502.

14) Agnello, M. *et al.* (2005) Evidence for a kaon-bound state K^-pp produced in K^- absorption reactions at rest. Phys. Rev. Lett. **94**, 212303.

15) Kienle, P. *et al.* (2012) Role of $\Lambda(1405)$ in the Formation of $X = K^-pp$ Revealed in $pp \rightarrow X + K^+$ at 2.50 and 2.85 GeV. Eur. Phys. J. A **48**, 183.

16) Agakishiev, G. *et al.* (2012) Production of $\Sigma^\pm \pi^\mp p K^+$ in $p + p$ reactions at 3.5 GeV beam energy. Nucl. Phys. A **881**, 178–186.

17) Hassanvand, M., Kalantari, S.Z., Akaishi, Y. and Yamazaki, T. (2013) Theoretical analysis of $\Lambda(1405) \rightarrow (\Sigma\pi)^0$ mass spectra produced in $p + p \rightarrow p + \Lambda(1405) + K^+$ reactions. Phys. Rev. C Nucl. Phys. **87**, 055202; Hassanvand, M., Kalantari, S.Z., Akaishi, Y. and Yamazaki, T. (2013) Publisher's Note: Theoretical analysis of $\Lambda(1405) \rightarrow (\Sigma\pi)^0$ mass spectra produced in $p + p \rightarrow p + \Lambda(1405) + K^+$ reactions [Phys. Rev. C 87, 055202 (2013)]. Phys. Rev. C Nucl. Phys. **88**, 019905(E).

18) Suzuki, K. *et al.* (2013) Studies of the exclusive

strangeness production reaction $pp \to p\Lambda K^+$ with DISTO at $T_p = 2.50$ and $2.85\,$GeV. (to be published).

19) Yamazaki, T., Akaishi, Y. and Hassanvand, M. (2011) New way to produce dense double-anti-kaonic dibaryon system, $\bar{K}\bar{K}NN$, through $\Lambda(1405)$-doorway sticking in $p + p$ collisions. Proc. Jpn. Acad., Ser. B **87**, 362–370.

20) Hassanvand, M., Akaishi, Y. and Yamazaki, T. (2011) Formation of K^-K^-pp in high-energy proton-proton collisions. Phys. Rev. C Nucl. Phys. **84**, 015207.

21) Kaplan, D.B. and Nelson, A.E. (1986) Strange goings on in dense nucleonic matter. Phys. Lett. B **175**, 57–63.

22) Brown, G.E., Lee, C.H., Rho, M. and Thorsson, V. (1994) From kaon-nuclear interactions to kaon condensation. Nucl. Phys. A **567**, 937–956.

23) Brown, G.E. and Bethe, H.A. (1994) A scenario for a large number of low-mass black holes in the galaxy. Astrophys. J. **423**, 659–664.

24) Beringer, J. *et al.* (Particle Data Group) (2012) Review of particle physics. Phys. Rev. D Part. Fields Gravit. Cosmol. **86**, 010001.

25) Esmaili, J., Akaishi, Y. and Yamazaki, T. (2010) Experimental confirmation of the $\Lambda(1405)$ ansatz from resonant formation of a K^-p quasi-bound state in K^- absorption by ^{3}He and ^{4}He. Phys. Lett. **686**, 23–28.

26) Esmaili, J., Akaishi, Y. and Yamazaki, T. (2011) Resonant formation of $\Lambda(1405)$ by stopped-K^- absorption in the deuteron. Phys. Rev. C Nucl. Phys. **83**, 055207.

27) Hyodo, T. and Weise, W. (2008) Effective $\bar{K}N$ interaction based on chiral SU(3) dynamics. Phys. Rev. C Nucl. Phys. **77**, 035204.

28) Doté, A., Hyodo, T. and Weise, W. (2009) Variational calculation of the ppK^- system based on chiral SU(3) dynamics. Phys. Rev. C Nucl. Phys. **79**, 014003.

29) Barnea, N., Gal, A. and Liverts, E.Z. (2012) Realistic calculations of $\bar{K}NN$, $\bar{K}NNN$, and $\bar{K}\bar{K}NN$ quasi-bound states. Phys. Lett. B **712**, 132–137.

30) Kienle, P. and Yamazaki, T. (2004) Pions in nuclei, a probe of chiral symmetry restoration. Prog. Part. Nucl. Phys. **52**, 85–132.

31) Suzuki, K. *et al.* (2004) Precision spectroscopy of pionic 1s states of Sn nuclei and evidence for partial restoration of chiral symmetry in the nuclear medium. Phys. Rev. Lett. **92**, 072302.

32) Yamazaki, T., Hirenzaki, S., Hayano, R.S. and Toki, H. (2012) Deeply bound pionic states in heavy nuclei. Phys. Rep. **514**, 1–87.

33) Faddeev, L.D. (1960) Scattering theory for a three-particle system. ZhETF **39**, 1459.

34) Yakubovsky, O.A. (1967) On the integral equations in the theory of N particle scattering. Sov. J. Nucl. Phys. **5**, 937; Faddeev, L.D. (1970) Three-Body Problem in Nuclear and Particle Physics (eds. McKee, J.S.C. and Rolph, R.M.). North-Holland, Amsterdam.

35) Kamada, H. *et al.* (2001) Benchmark test calculation of a four-nucleon bound state. Phys. Rev. C Nucl. Phys. **64**, 044001.

36) Filikhin, I.N. and Gal, A. (2002) Faddeev-Yakubovsky calculations for light $\Lambda\Lambda$ hypernuclei. Nucl. Phys. A **707**, 491–509.

37) Shevchenko, N.V., Gal, A. and Mares, J. (2007) Faddeev calculation of a K^-pp quasi-bound state. Phys. Rev. Lett. **98**, 082301.

38) Shevchenko, N.V., Gal, A., Mares, J. and Révai, J. (2007) $\bar{K}NN$ quasibound state and the $\bar{K}N$ interaction: Coupled-channels Faddeev calculations of the $\bar{K}NN - \pi\Sigma N$ system. Phys. Rev. C Nucl. Phys. **76**, 044004.

39) Ikeda, Y. and Sato, T. (2007) Strange dibaryon resonance in the $\bar{K}NN - \pi YN$ system. Phys. Rev. C Nucl. Phys. **76**, 035203.

40) Ikeda, Y. and Sato, T. (2009) Resonance energy of the $\bar{K}NN - \pi YN$ system. Phys. Rev. C Nucl. Phys. **79**, 035201.

41) Ikeda, Y., Kamano, H. and Sato, T. (2010) Energy dependence of $\bar{K}N$ interactions and resonance pole of strange dibaryons. Prog. Theor. Phys. **124**, 533–539.

42) Alt, E.O., Grassberger, P. and Sandhas, W. (1967) Reduction of the three-particle collision problem to multi-channel two-particle Lippmann-Schwinger equations. Nucl. Phys. B **2**, 167–180.

43) Sofianos, S., McGurk, N.J. and Fiedeldey, H. (1979) Energy-dependent pole expansions for the effective potentials in the four-body integral equations. Nucl. Phys. A **318**, 295–303.

44) Nakaichi, S., Lim, T.K., Akaishi, Y. and Tanaka, H. (1982) ^{4}He tetramer and the Faddeev-Yakubovsky theory. Phys. Rev. A **26**, 32–41.

45) Narodetsky, I.M. (1974) The integral equation approach to four-nucleon bound states. Nucl. Phys. A **221**, 191–210.

46) Filikhin, I.N., Yakovlev, S.L., Roudnev, V.A. and Vlahovic, B. (2002) The ^{4}He tetramer ground state in the Faddeev-Yakubovsky differential equations formalism. J. Phys. B: At. Mol. Opt. Phys. **35**, 501–508.

47) Akaishi, Y., Myint, K.S. and Yamazaki, T. (2008) Kaonic nuclear systems $\bar{K}N$ ans $\bar{K}NN$ as decaying states. Proc. Jpn. Acad., Ser. B **84**, 264–273.

48) Alston, M.H., Alvarez, L.W., Eberhard, P. and Good, M.L. (1961) Study of resonances of the $\Sigma - \pi$ system. Phys. Rev. Lett. **6**, 698–702.

49) Bastien, P., Ferro-Luzzi, M. and Rosenfeld, A.H. (1961) Sigma decay modes of pion-hyperon resonances. Phys. Rev. Lett. **6**, 702–705.

50) Dalitz, R.H. and Tuan, S.F. (1959) The energy dependence of low energy K^--proton processes. Ann. Phys. **8**, 100–118.

51) Nogami, Y. (1963) Possible existence of $\bar{K}NN$ bound states. Phys. Lett. **7**, 288–289.

52) Gal, A. (2007) Overview of $\bar{K}$-nuclear quasi-bound states. Nucl. Phys. A **790**, 143c–150c.

53) Bayar, M., Yamagata-Sekihara, J. and Oset, E. (2011) Overview of $\bar{K}$-nuclear quasi-bound states. Phys. Rev. C Nucl. Phys. **84**, 015209.

54) Akaishi, Y. (1986) Few-body system in realistic

interaction. Int. Rev. Nucl. Phys. **4**, 259–393.

55) Kanada-En'yo, Y. and Jido, D. (2008) $\bar{K}\bar{K}N$ molecular state in a three-body calculation. Phys. Rev. C Nucl. Phys. **78**, 025212.

56) Bethe, H. (1971) Theory of nuclear matter. Annu. Rev. Nucl. Sci. **21**, 93–244.

57) Akaishi, Y., Doté, A. and Yamazaki, T. (2005) Strange tribaryons as $\bar{K}$-mediated dense nuclear systems. Phys. Lett. B **613**, 140–147.

58) Nambu, Y. and Jona-Lasinio, G. (1961) Dynamical model of elementary particles based on an analogy with superconductivity. I. Phys. Rev. **122**, 345–358; Nambu, Y. and Jona-Lasinio, G. (1961) Dynamical model of elementary particles based on an analogy with superconductivity. II. Phys. Rev. **124**, 246–254.

59) Weinberg, S. (1966) Pion scattering lengths. Phys. Rev. Lett. **17**, 616–621.

60) Tomozawa, Y. (1966) Axial-vector coupling constant renormalization and the meson-baryon scattering lengths. Nuovo Cim., A **46**, 707–717.

61) Gell-Mann, M., Oakes, R.J. and Renner, B. (1966) Behavior of current divergences under $SU_3 \times SU_3$. Phys. Rev. **175**, 2195–2199.

62) Hatsuda, T. and Kunihiro, T. (1985) Fluctuation effects in hot quark matter: Precursors of chiral transition at finite temperature. Phys. Rev. Lett. **55**, 158–161.

63) Hatsuda, T. and Kunihiro, T. (1994) QCD phenomenology based on a chiral effective Lagrangian. Phys. Rep. **247**, 221–367.

64) Waas, T., Kaiser, N. and Weise, W. (1996) Low energy $\bar{K}N$ interaction in nuclear matter. Phys. Lett. B **365**, 12–16; Waas, T., Kaiser, N. and Weise, W. (1996) Effective kaon masses in dense nuclear and neutron matter. Phys. Lett. B **379**, 34–38.

65) Kaiser, N., Siegel, P.B. and Weise, W. (1995) Chiral dynamics and the low-energy kaon-nucleon interaction. Nucl. Phys. A **594**, 325–345.

66) Hayano, R.S. and Hatsuda, T. (2010) Hadron properties in the nuclear medium. Rev. Mod. Phys. **82**, 2949–2990.

67) Reinders, L.J., Rubinstein, H. and Yazaki, S. (1985) Hadron properties from QCD sum rules. Phys. Rep. **127**, 1–97.

68) Brown, G.E., Kubodera, K. and Rho, M. (1987) Strangeness condensation and "clearing" of the vacuum. Phys. Lett. B **192**, 273–278.

69) Kienle, P. (2007) Experimental studies of antikaon mediated nuclear bound systems. Int. J. Mod. Phys. A **22**, 365–373.

70) Zmeskal, J., Büler, P., Cargnelli, M., Ishiwatari, T., Kienle, P., Marton, J., Suzuki, K. and Widman, E. (2009) Double-strangeness production with antiprotons. Hyperfine Interact. **194**, 249–254.

71) Herrmann, N. (2013) FOPI experiments (private communication).

72) Yamazaki, T. (2012) Toward cold and dense antikaonic nuclear clusters—Talk at symposium "Creativity-Innovation—the seed for frontier science" on the occasion of the 80th birthday of Professor Paul Kienle. Hyperfine Interact. **211**, 69–75.